JCIM JOURNAL OF CHEMICAL INFORMATION AND MODELING

pubs.acs.org/jcim Article

In Silico Classifiers for the Assessment of Drug Proarrhythmicity

Jordi Llopis-Lorente, Julio Gomis-Tena, Jordi Cano, Lucía Romero, Javier Saiz, and Beatriz Trenor*

Cite This: *J. Chem. Inf. Model.* 2020, 60, 5172–5187 Read Online

ACCESS | Metrics & More | Article Recommendations | Supporting Information

ABSTRACT: Drug-induced torsade de pointes (TdP) is a life-threatening ventricular arrhythmia responsible for the withdrawal of many drugs from the market. Although currently used TdP risk-assessment methods are effective, they are expensive and prone to produce false positives. In recent years, *in silico* cardiac simulations have proven to be a valuable tool for the prediction of drug effects. The objective of this work is to evaluate different biomarkers of drug-induced proarrhythmic risk and to develop an *in silico* risk classifier. Cellular simulations were performed using a modified version of the O'Hara et al. ventricular action potential model and existing pharmacological data (IC_{50} and effective free therapeutic plasma concentration, EFTPC) for 109 drugs of known torsadogenic risk (51 positive). For each compound, four biomarkers were tested: T_x (drug concentration leading to a 10% prolongation of the action potential over the EFTPC), T_{qNet} (net charge carried by ionic currents when exposed to 10 times the EFTPC with respect to the net charge in control), T_{triang} (triangulation for a drug concentration of 10 times the EFTPC over triangulation in control), and T_{EAD} (drug concentration originating early afterdepolarizations over EFTPC). Receiver operating characteristic (ROC) curves were built for each biomarker to evaluate their individual predictive quality. At the optimal cutoff point, accuracies for T_x, T_{qNet}, T_{triang}, and T_{EAD} were 89.9, 91.7, 90.8, and 78.9% respectively. The resulting accuracy of the hERG IC_{50} test (current biomarker) was 78.9%. When combining T_x, T_{qNet} and T_{triang} into a classifier based on decision trees, the prediction improves, achieving an accuracy of 94.5%. The sensitivity analysis revealed that most of the effects on the action potential are mainly due to changes in I_{Kr}, I_{CaL}, I_{NaL} and I_{Ks}. In fact, considering that drugs affect only these four currents, TdP risk classification can be as accurate as when considering effects on the seven main currents proposed by the CiPA initiative. Finally, we built a ready-to-use tool (based on more than 450 000 simulations), which can be used to quickly assess the proarrhythmic risk of a compound. In conclusion, our *in silico* tool can be useful for the preclinical assessment of TdP-risk and to reduce costs related with new drug development. The TdP risk-assessment tool and the software used in this work are available at https://riunet.upv.es/handle/10251/136919.

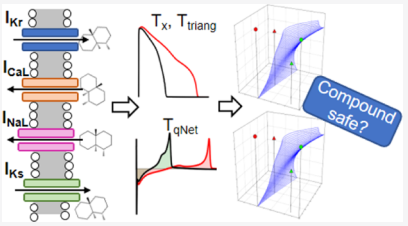

1. INTRODUCTION

Drug-induced torsade de pointes (TdP) is a life-threatening arrhythmia characterized by a gradual change in the amplitude and twisting of the QRS complexes.[1] It is one of the most feared adverse drug reactions. In fact, several compounds, without heart-related therapeutic indications, have been withdrawn from the market due to their ability to induce TdP.[2] Thus, the evaluation of proarrhythmic risk is considered an important public health problem and is receiving attention from governments, regulatory authorities, and pharmacological companies because of its socio-economic consequences.

In the 1990s, it was recognized that the induction of TdP was highly correlated with the pharmacological blockade of the human ether-à-go-go-related gene (hERG) channel (which mediates the rapid component of delayed rectifier current, I_{Kr}) and a prolongation of the QT interval.[3] As a consequence, two regulatory guidelines (S7B, non clinical guidance, and E14, clinical guidance) were established by the International Council on Harmonization (ICH) for cardiac risk assessment. These protocols have been successful in preventing torsadogenic drugs from being commercialized.[4] However, by focusing exclusively on hERG blockade and QT prolongation, they have also contributed to discarding from the development pipeline a large number of potentially useful compounds. Indeed, many studies[5,6] have shown that there are drugs, such as verapamil, that produce a hERG block but do not lead to TdP. Other ion currents have also been shown to influence the appearance of TdP. Therefore, a more accurate method for the torsadogenic risk assessment at the early stages of drug development, which takes into account multichannel interactions, would be of paramount importance for safety pharmacology.

Over the last years, biophysical models and computational simulations have been widely used to improve the prediction of drug cardiotoxicity. New international paradigms for the proarrhythmic assessment of drugs, such as the Comprehensive *in vitro* Proarrhythmia Assay (CiPA), consider that *in silico* simulations of proarrhythmic effects for different compounds have a key role in linking data from *in vitro* assays to changes in cell behavior and are essential to improve

Received: March 16, 2020
Published: July 27, 2020

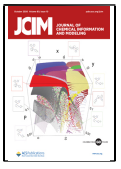

Table 1. TdP-Risk Classification of the 109 Drugs Used in This Study[a]

Compound Name	Class	Compound Name	Class	Compound Name	Class
Ajmaline	1*	Pimozide	1	Deferasirox	4*
Amiodarone	1	Clozapine	2	Desvenlafaxine	4
Astemizole	1	Desipramine	2	Diazepam	4
Azithromycin	1	Dolasetron	2	Diltiazem	4
Bepridil	1	Lapatinib	2	Doxorubicin	4
Chloroquine	1	Lopinavir	2	Duloxetine	4
Chlorpromazine	1	Nilotinib	2	Ebastine	4*
Cilostazol	1	Paliperidone	2	Eltrombopag	4
Cisapride	1	Risperidone	2	Etravirine	4*
Clarithromycin	1	Ritonavir	2	Everolimus	4
Disopyramide	1	Saquinavir	2	Lamivudine	4
Dofetilide	1	Sertindole	2	Lidocaine	4
Domperidone	1	Sunitinib	2	Linezolid	4
Donepezil	1	Tolterodine	2	Loratadine	4
Dronedarone	1	Tamoxifen	2	Maraviroc	4*
Droperidol	1	Amitriptyline	3	Metoprolol	4
Erythromycin	1	Diphenhydramine	3	Mexiletine	4
Flecainide	1	Famotidine	3	Mibefradil	4*
Gatifloxacin	1	Fluvoxamine	3	Mitoxantrone	4
Halofantrine	1	Metronidazole	3	Nebivolol	4
Haloperidol	1	Nelfinavir	3	Nifedipine	4
Ibutilide	1	Paroxetine	3	Nitrendipine	4*
Levofloxacin	1	Propafenone	3	Nisoldipine	4*
Methadone	1	Quetiapine	3	Oxybutynin	4
Moxifloxacin	1	Quinine	3	Palonosetron	4
Ondansetron	1	Ranolazine	3	Pentobarbital	4*
Procainamide	1	Solifenacin	3	Phenytoin	4
Quinidine	1	Voriconazole	3	Propranolol	4
Sotalol	1	Alvimopan	4*	Raltegravir	4
Sparfloxacin	1	Ambrisentan	4	Ribavirin	4
Tedisamil	1*	Aspirin	4	Rufinamide	4*
Terfenadine	1	Ceftriaxone	4	Sildenafil	4
Terodiline	1	Chlorpheniramine	4	Silodosin	4
Thioridazine	1	Cibenzoline	4*	Sitagliptin	4*
Azimilide	1*	Darifenacin	4	Tadalafil	4
Vandetanib	1	Darunavir	4	Telbivudine	4*
				Verapamil	4

[a]Each drug is color-coded according to its torsadogenic risk: red for class 1 (known risk of TdP), orange for class 2 (possible risk of TdP), yellow for class 3 (conditional risk of TdP), green for class 4 (drugs with a lack of evidence of TdP). An asterisk indicates that the drug was not in the CredibleMeds list and was assigned to a class according to the literature.

arrhythmogenicity prediction.[4,7] Numerous *in silico* classifications tools have been published,[8−14] which have shown to improve TdP risk assessment and are gradually becoming an alternative to reduce animal experiments during the early stages of drug development. These *in silico* evaluations are based on performing different simulations (reported studies use single-cell models, one-dimensional models, or even whole-heart simulations) to calculate a set of features such as action potential duration, diastolic calcium, or transmural dispersion of repolarization, among others, and use them for TdP risk discrimination. These strategies have demonstrated the capability to make good predictions;[8,15−17] however, there is still space for improvement, since they still present some limitations, such as a reduced number of compounds, considering drug effects on just a small number of ion channels, and usage of non updated biophysical models, among others. Hence, the development of new TdP risk-assessment methods based on *in silico* simulations can be of high interest.

In previous work, our group developed a method for the early screening of drug-induced proarrhythmic risk. It consists of four matrices that, taking into account blocking effects on I_{Kr}, I_{CaL}, and I_{Ks}, provide the value of an arrhythmogenic index called T_x, predicting whether the drug is proarrhythmic.[10] It was successfully tested in 84 compounds, at that time, one of the largest drug databases employed. The method was implemented in the QT/TdP risk screen tool available on

https://dx.doi.org/10.1021/acs.jcim.0c00201
J. Chem. Inf. Model. 2020, 60, 5172−5187

the web-based InSilicoTrials.com platform (www.insilicotrials.com) built in the Microsoft Azure cloud environment, in compliance with the highest standards of security and privacy. The aims of this study are (i) to improve our *in silico* classifier for the assessment of TdP risk by taking into account the seven ionic currents selected by the CiPA initiative due to their important role in arrhythmogenesis (I_{Na}, I_{NaL}, I_{Kr}, I_{to}, I_{CaL}, I_{K1}, and I_{Ks}), increase our database, define new effective biomarkers, and use different machine-learning tools to achieve a more reliable and robust prediction and (ii) to identify the ionic currents that have the most significant impact on TdP risk prediction. This will help in reducing the amount of *in vitro* experiments necessary to characterize a drug and simulate its effect, thus accelerating the process of drug development and reducing the associated costs.

2. MATERIALS AND METHODS

2.1. Cellular *In Silico* Simulations. The electrophysiological characteristics of human ventricular cells were simulated using a modified version of the human endocardial ventricular action potential (AP) model published by O'Hara et al.[18] The O'Hara et al. model is one of the most recent and used *in silico* AP models.[19,20] In fact, it was proposed by the CiPA initiative as the starting point for the development of *in silico* tools for regulatory decision-making.[4] However, the O'Hara et al. model[18] still has some issues that should be addressed.[21] In this work, the model modifications include a modulation of five channel conductances according to Dutta et al.,[22] a reformulation of the activation and inactivation gates of I_{Na}, and a reduction of its conductance by 60%.[20,23] The modification in channel conductances was carried out, aiming at better reproducing experimental data of drug effects. As suggested by Dutta el al.,[22] the following conductances were scaled: I_{Kr} by 1.119, I_{Ks} by 1.648, I_{K1} by 1.414, I_{CaL} by 1.018, and I_{NaL} by 2.274. For further details about the equations describing I_{Na} dynamics, see Table S1 in the Supporting information.

Drug effects on the AP were simulated via the simple pore block model, as in previous studies.[9,10,16,24] Thus, the block produced on each current was simulated by scaling the channel's maximal conductance (g_i). This scaling factor was calculated using the standard Hill equation (eq 1). In this work we considered drug effects on the seven ionic currents selected by the Ion Channel Working Group of the CiPA initiative for playing the most important role in the generation of the AP and cardiac arrhythmias (I_{Na}, I_{NaL}, I_{Kr}, I_{to}, I_{CaL}, I_{K1}, and I_{Ks}).[4,7]

$$g_{i,\mathrm{drug}} = g_i\left[1 + \left(\frac{D}{\mathrm{IC}_{50,i}}\right)^h\right]^{-1} \quad (1)$$

where $g_{i,\mathrm{drug}}$ is the maximal conductance of channel i in the presence of the drug, D is the drug concentration, $\mathrm{IC}_{50,i}$ is the half-maximal response dose for that drug and current through channel I, and h is the Hill coefficient indicating the number of molecules of the drug that are assumed to be sufficient to block one ion channel.

All simulations were carried out with a basic cycle length (BCL) of 1000 ms and a stimulus of 1.5-fold the diastolic threshold of amplitude and a duration of 0.5 ms. Measurements of indices and biomarkers were done once the steady state (after 1000 beats starting from control—no drug—steady-state initial values) was achieved.

2.2. Drugs Data Set. In this work, we assessed the proarrhythmic risk of 109 drugs using derived features (parameters obtained from biophysical models and explained in detail in Section 2.3). For these compounds, the ground truth was taken from CredibleMeds.[25] CredibleMeds classification is based on an extensive search of both the literature and public databases, which is continuously updated in light of new evidence and is recognized by the clinical community.

This database defines four drug-induced TdP risk categories: class 1, compounds that prolong the QT interval and are clearly associated with a known risk of TdP, even when taken as recommended; class 2, compounds with a possible risk of TdP; class 3, drugs associated with TdP but only under certain conditions (excessive dose, interactions, patients with pathological conditions, etc.); and class 4, drugs with a lack of evidence to be placed in any of the other classes. The classification of the 109 drugs studied in this work is provided in Table 1. In this work, for the purpose of developing binary classifiers, we grouped together classes 1 and 2 as TdP+ and 3 and 4 as TdP−.

Ajmaline, tedisamil and azimilide are not included in the CredibleMeds classification, but they were included in class 1 according to Mirams et al.,[16] Romero et al.,[10] and Fermini et al.[7] Other drugs (marked with an asterisk in Table 1) that are not included in CredibleMeds and with a lack of evidence of TdP were considered as class 4 (as in Romero et al.[10]).

For each of these 109 drugs, IC_{50} values and Hill coefficients (h) for I_{Na}, I_{NaL}, I_{Kr}, I_{to}, I_{CaL}, I_{K1}, and I_{Ks} and human effective free therapeutic plasma concentration (EFTPC) were obtained from either public databases, like DrugBank, DailyMed, or PubChem, or the scientific literature, always avoiding data extracted from Xenopus oocytes. EFTPC values were used directly from the source (when available) or calculated taking into account the protein-bound fraction and the peak plasma concentrations (see Supporting information, Table S2). When multiple IC_{50} were presented, we considered that all published data represented a distribution of values affected by a random error. To deal with that variability and summarize this distribution in a robust value, the value at the center of the distribution was selected (i.e., the median value). For the Hill coefficient, we took the one associated with the median IC_{50} value chosen. In those cases when no IC_{50} value were found, the block of the corresponding channel was not considered in our simulations. When several EFTPC values where found, we considered the worst-case scenario by selecting the value for the highest dose. The EFTPC, IC_{50}, and Hill coefficient values for the 109 drugs are listed in the Supporting information, Table S2.

2.3. Torsadogenic Indices. In recent years, various "derived features" have been proposed for the assessment of drug proarrhythmicity. Derived features are parameters or indices obtained from biophysical computational models and have proven to be promising metrics to provide a mechanism-based classification of compounds. Furthermore, they have the potential to lead to a replacement of animal experiments in the early phases of drug development.[26] In Parikh and colleagues,[24,26] a brief review of the *in silico* arrhythmogenic biomarkers proposed over the last years can be found. In this work, we have studied four different torsadogenic indices (see Figure 1).

2.3.1. T_x. This arrhythmogenic index was proposed by Romero et al.[10] and tested in 84 drugs, providing a classification accuracy of 88%. It is defined as the ratio

https://dx.doi.org/10.1021/acs.jcim.0c00201
J. Chem. Inf. Model. 2020, 60, 5172−5187

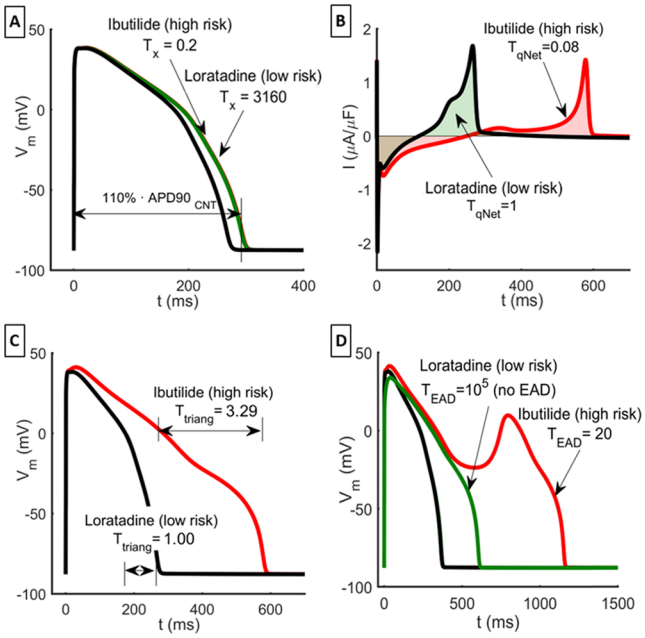

Figure 1. Studied arrhythmogenic indices. Curves corresponding to simulations in control conditions are represented in black; red curves represent AP under effects of a high-proarrhythmic-risk drug (ibutilide), while green ones represent effects under a low-proarrhythmic-risk drug (loratadine). (A) T_x index. The AP under drug effects with an APD_{90} 10% longer than the control APD_{90} is represented. Traces for low- and high-risk drugs are overlapped, but the concentration needed to achieve a 10% APD_{90} prolongation is much higher in the case of the low-risk drug and thus T_x is much greater. (B) Charge carried by I_{net}. The area under the I_{net} curve for the last beat when the low-risk drug is applied at a concentration of 10 times the EFTPC is plotted in green. The area under the I_{Net} curve for the high-risk one is plotted in red. (C) T_{triang} index. APs under 10 times the EFTPC are traced for a torsadogenic drug and for a nontorsadogenic drug. Ibutilide (high risk) has a greater impact on the AP, producing a longer triangulation. Loratadine (low risk) and control curves are coincident because the effect of loratadine at those concentrations on the AP is negligible. (D) T_{EAD} index. AP curves at the dose generating EAD are represented. When the high-risk drug is applied at 20 times the EFTPC, it provokes an EAD (positive voltage gradient during the repolarization phase). For the low risk drug, there is no EAD even at 10^5 times the EFTPC.

between the concentration of a drug that provokes a 10% prolongation of the action potential duration at 90% repolarization (APD_{90}) in control conditions and the EFTPC. Therefore, a high T_x value means that the concentration needed to increase APD_{90} by 10% is much higher than the EFTPC and thus the drug is safe. In Figure 1A, AP in control conditions (black line) and AP with a 10% APD_{90} prolongation due to drug effects are shown. It can be seen that safe drugs (such as loratadine, plotted in green) have a greater T_x value than proarrhythmic drugs (such as ibutilide, plotted in red) because their effect on APD prolongation is weak and the concentration needed to prolong APD_{90} by 10% is much higher.

$$T_x = \frac{[D]_{APD\uparrow 10\%}}{EFTPC} \quad (2)$$

2.3.2. T_{qNet}. This index is based on the concept of qNet (net charge) that was proposed in Dutta et al.[15] qNet is calculated as the area under the curve traced by the net current (I_{net} = I_{CaL}+ I_{NaL}+ I_{Kr} + I_{Ks} + I_{K1} + I_{to}) during a whole beat. This index was able to separate with accuracy the 12 training CiPA drugs into the desired target groups. In addition, Li et al.[5] used the qNet value averaged across 1−4 × C_{max} and successfully predicted the TdP risk of 16 test compounds.[5] Here, we define T_{qNet} as the ratio between the net charge carried by I_{net} when exposed to 10 times the EFTPC with respect to the net charge in control conditions (eq 3). For a given drug, a T_{qNet} near 1 means that the net charge at 10 times the EFTPC is very similar to the net charge at control conditions. Values higher than 1 indicate an increase in repolarization reserve, and therefore safety;[27] on the contrary, low values of T_{qNet} are associated with a higher propensity of TdP. In Figure 1B, the net current for the last beat under 10 times the EFTPC concentration of loratadine (low-risk drug) is plotted in green and the net current under 10 times the EFTPC concentration of ibutilide (high-risk drug) in red. It can be observed that torsadogenic drugs have less net charge with respect to control condition and consequently smaller T_{qNet}. Ten times the EFTPC concentration was chosen to distinguish drug effects without being an excessively high dose.

$$T_{qNet} = \frac{qNet_{at10\times\ EFTPC}}{qNet_{control}} \quad (3)$$

2.3.3. T_{triang}. This index is the ratio between triangulation (APD_{90}−APD_{30}) for a drug concentration of 10 times EFTPC and triangulation in control (eq 4). Similar to that of T_{qNet}, values near 1 mean that the triangulation at 10 times the EFTPC is practically equal to triangulation at control conditions. However, in this case, as torsadogenic drugs produce more changes in the morphology of AP and prolong its duration, its T_{triang} is expected to be greater than 1. Specifically, higher T_{triang} means that the drug affects more in the repolarization phase, originating a lower repolarization reserve, which is related to the development of TdP.[27] In Figure 1C, changes in AP at 10 times the EFTPC of loratadine and ibutilide are represented. Ibutilide has a greater impact on the AP, producing a longer triangulation, while loratadine effects on AP at that concentration are negligible, being equal to those of the AP control.

$$T_{triang} = \frac{(APD_{90} - APD_{30})_{at\ 10\times\ EFTPC}}{(APD_{90} - APD_{30})_{control}} \quad (4)$$

2.3.4. T_{EAD}. This index measures the likelihood to develop an early afterdepolarization (EAD), which is thought to be a key determinant for TdP development.[28] It is defined as the ratio between the drug concentration needed to originate an EAD or a repolarization failure and the EFTPC (eq 5). Thus, the lower the T_{EAD}, the higher ability of the drug to induce EADs or repolarization failures and the more dangerous the drug. An EAD was defined as any event with a positive voltage gradient ($dV/dt > 0$ms) after 100 ms from the beginning of the AP. It was considered that there was a repolarization failure when the membrane voltage at the end of the beat was higher than the resting membrane voltage (V_m > −40 mV). The stimulation protocol for the generation of EADs and repolarization failures was similar to that used by Viswanathan and Rudy:[29] for a given drug concentration, 999 stimuli at a 1 Hz BCL were simulated, then a 2000 ms pause was taken, and an extra stimulus was applied. The drug concentration was gradually increased from EFTPC until an EAD appeared or until 10^5 times the EFTPC. If no EAD appeared at this

https://dx.doi.org/10.1021/acs.jcim.0c00201
J. Chem. Inf. Model. 2020, 60, 5172−5187

concentration, the T_{EAD} was considered 10^5. Traces of AP at drug concentrations producing EADs are shown in Figure 1D. An EAD can be observed when ibutilide is applied at 20 times the EFTPC (red line), while in the case of loratadine (green line), even at 10^5 times the EFTPC, there is no EAD (although it increases APD with respect to the control—black line).

$$T_{EAD} = \frac{[D]_{EADs}}{EFTPC} \quad (5)$$

All indices were analyzed for the last beat in simulations of 1000 beats.

2.4. Sensitivity Analysis. One of the objectives of this work is to determine the currents that have more influence on the prediction of cardiotoxicity. In this sense, we performed a sensitivity analysis following a similar methodology to that proposed by Britton et al.[30] Briefly, first, we generated a population of 1000 virtual drugs. We considered the virtual drugs affecting the seven most arrhythmogenic currents according to the CiPA initiative (I_{Na}, I_{NaL}, I_{Kr}, I_{to}, I_{CaL}, I_{K1}, and I_{Ks}). Thus, a virtual drug consists of a set of seven scale factors (one for each ionic current) between ±60%. This range includes the vast majority of inhibition or enhancement effects that drugs usually have at therapeutic concentrations. The parameter sets of scaling factors were obtained using Latin hypercube sampling (LHS). After running simulations with the virtual drugs, the biomarkers were computed, and the partial correlation coefficients (PCC) method was applied, relating the indices to the currents. As they are virtual drugs and their EFTPCs are not known, the biomarkers calculated were surrogates of the four indices proposed. They were APD_{90} (a surrogate of T_x), T_{qNet_mod} (qNet at the effect of the virtual drug over the qNet control, as EFTPC was not known), and T_{triang_mod} (triangulation at the effect of the virtual drug over the triangulation control).

We also tested the other two methodologies to perform the sensitivity analysis. After a population of virtual drugs using a log-normal distribution of scaling factors between ±60% was obtained, the simulations were run and the biomarkers computed. In one case, partial least square (PLS) regression using the NIPALS algorithm[31] was applied, and, in the other, a multiple linear regression[32] was performed.

Based on the results of this analysis, the proarrhythmic indices were recalculated, taking into account only the currents with a greater impact. These biomarkers were used to build new torsadogenic drug classifiers to study how the proarrhythmic prediction changed.

2.5. Torsadogenic Drug Classifier. Finally, we combined T_x, T_{qNet}, and T_{triang} indices into a unique classifier to analyze whether the classification performance improves. The *in silico* TdP risk classifier was built using MATLAB (Mathworks Inc., Natwick, MA). First, a 9-fold cross-validation was applied. The original dataset (109 compounds) was randomly split into nine sets, and in each iteration, one of the sets (12 compounds) was left out as test series while the remaining nine sets (97 compounds) were used as training series. A classification decision tree was built using the training set in each iteration, thus yielding nine classification trees. For each decision tree, the maximum number of splits allowed was four. To obtain the output of the binary risk classifier, a majority voting technique[33] between the prediction of each decision tree was applied.

3. RESULTS

3.1. Predictive Performance of the Arrhythmogenic Indices. The value of each arrhythmogenic index for the 109 drugs studied in this work was calculated. The receiver operating characteristic (ROC) curves of the indices T_x (black), T_{qNet} (red), and T_{triang} (blue) are shown in Figure 2A. This figure also depicts the ROC curve for two metrics based on results from the hERG assay, which is currently used as a surrogate marker of TdP risk according to ICH S7B guidelines. These two metrics are pIC_{50} hERG (−log IC_{50} hERG) and hERG IC_{50}/EFTPC. It can be observed that the ROC curves for T_x, T_{qNet}, and T_{triang} are similar, with the areas under the curve (AUCs) being 0.94, 0.94, and 0.93, respectively. All of them are greater than the AUC for the metrics based on IC_{50} hERG, which are 0.90 for IC_{50} hERG/EFTPC and 0.82 for pIC_{50} hERG tests.

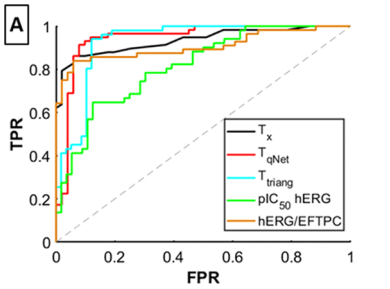

B

T_x	TdP+	TdP-
+	48	8
-	3	50
Acc:	TPR:	TNR:
89.9	0.94	0.86

T_{triang}	TdP+	TdP-
+	48	7
-	3	51
Acc:	TPR:	TNR:
90.8	0.94	0.88

T_{qNet}	TdP+	TdP-
+	46	4
-	5	54
Acc:	TPR:	TNR:
91.7	0.90	0.93

IC_{50} hERG / EFTPC	TdP+	TdP-
+	48	11
-	3	47
Acc:	TPR:	TNR:
87.2	0.94	0.81

Figure 2. (A) ROC curves for T_x (black), T_{qNet} (red), T_{triang} (blue), pIC_{50} hERG (green) and IC_{50} hERG/EFTPC (orange). The dashed line indicates the performance of a model that does not discriminate. (B) Confusion matrices for the arrhythmogenic indices at the optimal cutoff point (where sensitivity and specificity are maximal). Columns (TdP+ and TdP−) indicate the actual classification of the compounds (Table 1), and rows (+ and −) indicate the prediction made by the index studied. The cutoff points are 8 for T_x, 1.19 for T_{triang}, 0.88 for T_{qNet}, and 39 for IC_{50} hERG/EFTPC. True positives rates (TPR), true negatives rates (TNR), and accuracies (Acc) are also shown.

Figure 2B shows the confusion matrices for T_x, T_{qNet}, T_{triang}, and IC_{50} hERG/EFTPC indices at the optimal cutoff points, which is the threshold that achieves the nearest point to the upper-left corner of the ROC curve, where sensitivity and specificity are maximal. The optimal cutoff points were 8 for T_x, 1.19 for T_{triang}, 0.88 for T_{qNet}, and 39 for IC_{50} hERG/EFTPC. It can be highlighted that T_x, T_{qNet}, and T_{triang} tests led to very similar accuracies (around 90%), again higher than the performance of the pIC_{50} hERG and IC_{50} hERG/EFTPC tests. At the optimal cutoff point for the T_x test, 48 out of the 51 (94% specificity) torsadogenic drugs (class 1 and class 2, see Table 1) and 50 of the 58 (86% sensitivity) nontorsadogenic

https://dx.doi.org/10.1021/acs.jcim.0c00201
J. Chem. Inf. Model. 2020, 60, 5172−5187

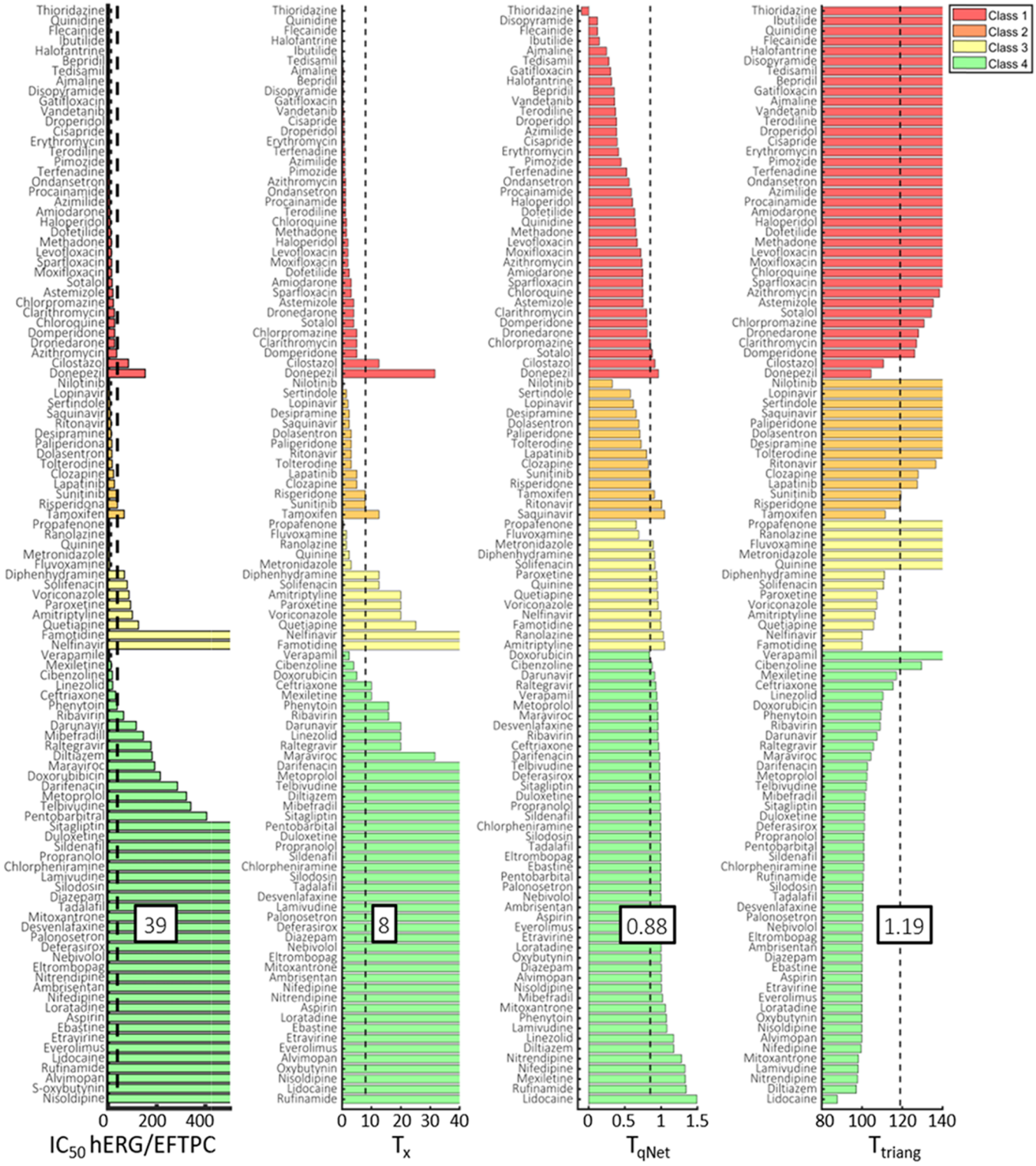

Figure 3. TdP risk classification of the 109 compounds with different proarrhythmic indices at the optimal cutoff point. The criterion was that drugs with hERG IC_{50}/EFTPC < 39, T_x < 8, T_{qNet} < 0.88, and T_{triang} > 1.19 were predicted as torsadogenic. Class 1 and 2 compounds are considered unsafe drugs, while class 3 and 4 compounds are considered safe drugs.

drugs (classes 3 and 4) were correctly classified. The performance for the decision T_{qNet} < 0.88 was as follows: a specificity (true negative rate) of 93% and a sensitivity (true positive rate) of 90%, leading to an accuracy of 91.7%. The T_{triang} test classified correctly 48 proarrhythmic and 51 nonproarrhythmic compounds, which corresponds to a sensitivity of 94% and a specificity of 88%. Regarding the metrics based on IC_{50} hERG, the accuracy obtained with the threshold IC_{50} hERG/EFTPC < 39 was 87.2%, classifying correctly 48 proarrhythmic compounds and 47 nonproarrhythmic compounds. For the test pIC_{50} hERG (not shown in the figure), at the optimal cutoff point (pIC_{50} hERG > 5.8), the resulting accuracy yielded 78.9%. With this test, 18 TdP+

https://dx.doi.org/10.1021/acs.jcim.0c00201
J. Chem. Inf. Model. 2020, 60, 5172−5187

drugs were considered as nontorsadogenic (65% of sensitivity) and five TdP− as torsadogenic (91% specificity).

Note that results for T_{EAD} were not included in this figure for the sake of clarity, as it was the index that performed the worst. Its performance was slightly lower than that of the pIC_{50} hERG, yielding an AUC of 0.80 and an accuracy at the optimal cutoff point of 78.9%. The resulting sensitivity was 73% (14 false-positive drugs) and the specificity was 85% (nine false-negative drugs).

Figure 3 shows the value of the indices IC_{50} hERG/EFTPC, T_x, T_{qNet}, and T_{triang} for the 109 drugs and the torsadogenic risk classification of these compounds using four different criteria to consider a drug as torsadogenic: IC_{50} hERG/EFTPC < 39, T_x < 8, T_{qNet} < 0.88, and T_{triang} > 119. According to the IC_{50} hERG/EFTPC test, cilostazol and donepezil, which are class 1 compounds (compounds with a known risk of TdP), and tamoxifen (class 2 compound) were predicted as safe drugs. For safe drugs, the IC_{50} hERG/EFTPC test misclassified five class 3 drugs (propafenone, ranolazine, quinine, metronidazole, and fluvoxamine) and six class 4 drugs (verapamil, mexiletine, cibenzoline, linezolid, ceftriaxone, and phenytoin). It is worth noting that T_x, T_{qNet}, and T_{triang} indeces misclassified as nontorsadogenic (false negative) the same two class 1 compounds, namely, cilostazol and donepezil, as well as tamoxifen, a class 2 compound (compounds with a possible risk of TdP). They also misclassified as torsadogenic the same two class 3 compounds (fluvoxamine and propafenone) and the same class 4 compound (cibenzoline). In addition, T_x and T_{triang} both misclassified metronidazole, quinine, and ranolazine (class 3 compounds), and the class 4 compound verapamil. T_x and T_{qNet} misclassified doxorubicin, a class 4 drug. T_{qNet} also misclassified as non torsadogenic class 2 drugs: ritonavir and saquinavir.

3.2. Sensitivity Analysis. Next, we wanted to analyze which of the seven CiPA currents have more effect on the electrophysiological characteristics of the AP. We simulated the effect of a population of 1000 virtual drugs and applied the partial correlation coefficients (PCC) method, as described in Section 2.4, to estimate the association between the arrhythmogenic indices and the seven currents. The effects of these virtual drugs on the AP and on the intracellular calcium transient are shown in Figure 4A,B. Control APs and calcium transients are plotted with a thick black line. It can be observed that some drugs shorten the AP, while others prolong it. For the intracellular calcium dynamics, it can also be observed that some drugs increase the amplitude of the calcium transient, while others decrease it. Thus, with this population of virtual drugs, we can represent a wide variety of pharmacological effects.

The PCC values for each current and biomarker are plotted in Figure 4C. For APD_{90}, the currents that have a higher PCC value are: I_{Kr} (−0.97), I_{NaL} (0.74), I_{CaL} (0.60), and I_{Ks} (−0.54). The I_{K1} coefficient is −0.47, and the other coefficients are lower than 0.14. For the T_{triang_mod} index, the currents with more influence are I_{Kr} (−0.96), I_{K1} (0.63), I_{NaL} (0.56), and I_{CaL} (−0.35). In this case, the PCC value for I_{Ks} is −0.25, for I_{Na} is −0.18, and for I_{to} is −0.11. For T_{qNet_mod}, the higher PCC values are for I_{Kr} (0.98), I_{NaL} (−0.98), I_{CaL} (−0.91), and I_{Na} (0.89). The other values are below 0.62, which is the I_{Ks} coefficient. It should be noted that the effects of I_{to} on the three biomarkers are practically negligible. If we add the three coefficients of each current in absolute value to represent the global relevance of each current in the value of the biomarkers,

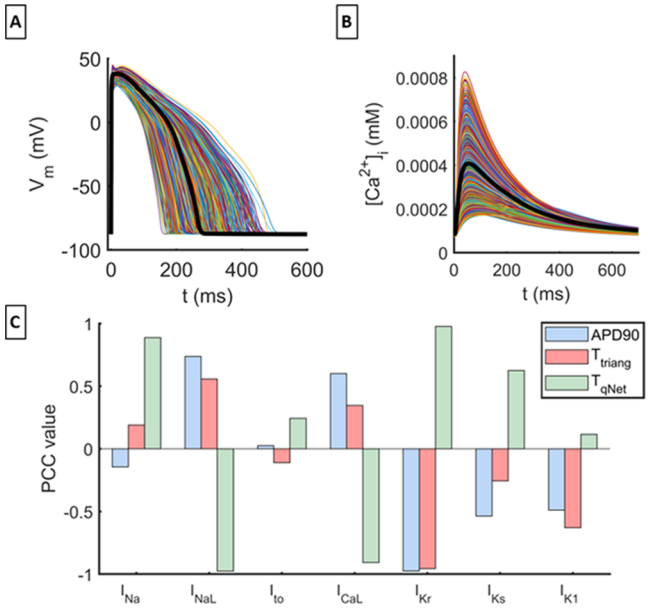

Figure 4. Results of sensitivity analysis. (A) Effects of the 1000 virtual drugs on the action potential. The black line represents the control AP. (B) Effects of the 1000 virtual drugs on intracellular calcium dynamics. The black trace corresponds to the control calcium transient. (C) PCC values of each of the seven CiPA drugs for APD_{90} (blue), T_{triang_mod} (red), and T_{qNet_mod} (green).

the currents yielding the highest values are I_{Kr} (2.91), I_{NaL} (2.27), I_{CaL}(1.85), and I_{Ks} (1.41). Thus, these results suggest that the currents that are globally more relevant to predict the torsadogenic effects of a drug are I_{Kr}, I_{CaL}, I_{NaL}, and I_{Ks}. It is true that the coefficient of I_{Na} for T_{qNet_mod} is higher than the I_{Ks} PCC coefficient, but for the other biomarkers, the influence of I_{Na} is smaller than the influence of I_{Ks}. For T_{triang_mod}, the I_{K1} PCC coefficient is also higher than the I_{Ks} PCC coefficient, but again, for the other biomarkers, I_{Ks} is more relevant.

In the Supporting information, the results of the sensitivity analysis using a multivariable linear regression (Figure S1) and the PLS method (Figure S2) are shown. Both methods obtain very similar coefficient values. It can be observed that the sign of the biomarker-ion current dependency (positive or negative) is the same with both sensitivity methods. In addition, the currents that have greater influence (greater value of the addition of three absolute values of the coefficients) are the same: I_{Kr}, I_{NaL}, I_{CaL}, and I_{Ks}. Therefore, according to our results, it can be deduced that regardless of the method used, qualitatively the same results are obtained. That is, the currents with the most significant global influence on TdP risk prediction biomarkers are I_{Kr}, I_{CaL}, I_{NaL}, and I_{Ks}.

3.3. Binary Torsadogenic Risk Classifiers. To improve the power of prediction, we combined T_x, T_{qNet}, and T_{triang} into a unique classifier. As described in Section 2.5, using the three proarrhythmogenic indices as inputs, we built nine decision trees. Each decision tree consisted of a maximum of four cutoff points. The cutoff points were calculated specifically for each decision tree, aiming to achieve optimal performance. Two of the nine decision trees that constitute this classifier are represented in Figure 5. The remaining decision trees are shown in Figure S3. For each drug, each tree takes several decisions and makes a prediction. For example, in tree 1 (Figure 5), the T_{qNet} index is evaluated first. If it is less than 0.91, then the next step is to evaluate T_{triang}. Depending on

https://dx.doi.org/10.1021/acs.jcim.0c00201
J. Chem. Inf. Model. 2020, 60, 5172−5187

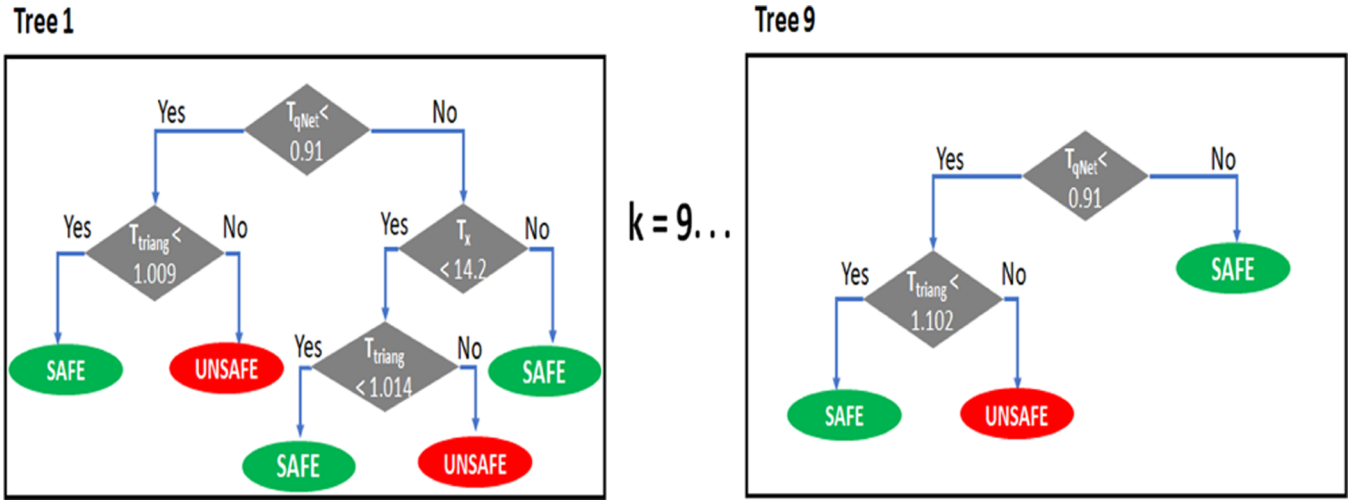

Figure 5. Two of the nine decision trees that constitute the binary TdP risk classifier. Each tree takes several decisions and makes a prediction. The final output of the classifier is obtained by taking into account the most voted class (safe or unsafe) among the nine decision trees.

Table 2. Performance of the Binary TdP Risk Classifier Depending on the Way of Calculating the Biomarkers Used as Input[a]

currents considered	Acc. (%)	false negatives (% sensitivity)	false positives (% specificity)
I_{Na}, I_{NaL}, I_{to}, I_{Kr}, I_{CaL}, I_{Ks}, and I_{K1}	94.5	3 (94%): donepezil, ritonavir, saquinavir	3 (95%): fluvoxamine, propafenone, cibenzoline
I_{Kr}, I_{CaL}, and I_{Ks}	92.7	1 (98%): cilostazol	7 (88%): fluvoxamine, propafenone, quinine, ranolazine, cibenzoline, mexiletine, and verapamil
I_{Kr}, I_{CaL}, and I_{NaL}	93.6	2 (96%): cilostazol, donepezil	5 (91%): metronidazole, propafenone, quinine, ranolazine, and verapamil
I_{Kr}, I_{CaL}, I_{Ks}, and I_{Kr}, I_{CaL}, I_{NaL}	94.5	3 (94%) milostazol, donepezil, sotalol	3 (95%) metronidazole, ranolazine, verapamil

[a]Four different classifiers have been built: one considering that drugs affect the seven CiPA currents; another considering effects on I_{Kr}, I_{CaL}, and I_{Ks}; another assuming effects on I_{Kr}, I_{CaL}, and I_{NaL}; and another combining biomarkers calculated taking into account effects on I_{Kr}, I_{CaL}, and I_{Ks} and biomarkers assuming effects on I_{Kr}, I_{CaL}, and I_{NaL}. The table indicates the accuracy of the classifier (Acc.), the false negatives, and the false positives.

whether T_{triang} is greater or smaller than 1.009, the tree predicts that the drug is safe or torsadogenic. On the contrary, if the drug has a T_{qNet} greater than 0.91, the other branch of the tree should be followed. Thus, after evaluating T_{qNet}, T_x is studied. Whether it is greater than 14.2, then the drug is safe. If not, T_{triang} has to be finally evaluated to decide if the drug will be safe or dangerous. The rest of the trees make a prediction in a similar way. Finally, the overall prediction of the classifier is made according to what has been the most voted class (safe or unsafe) among the nine decision trees.

The performance of this classifier is summarized in the first line of Table 2. The accuracy achieved by this classifier is 94.5%, which misclassifies only six drugs. The false negatives were donepezil, a class 1 drug, and ritonavir and saquinavir, two class 2 drugs, while the false positives were two class 3 drugs (fluvoxamine and propafenone) and one class 4 compound (cibenzoline). It should be noted that these drugs were also misclassified when using T_x, T_{qNet}, and T_{triang} individually as predictors.

Based on the sensitivity analysis, we also studied how the proarrhythmic prediction changed when simulating and calculating the biomarkers, assuming that drugs affected less currents (the ones with greater impact according to the sensitivity analysis). Thus, biomarkers were recalculated in two different ways: considering that drugs affect only I_{Kr}, I_{CaL}, and I_{Ks} and considering drug effects only on I_{Kr}, I_{CaL}, and I_{NaL}. This strategy was adopted because one of the objectives of the work is to provide a ready-to-use tool with the precalculated arrhythmogenic indices, implying a large amount of simulations combining blockade of three currents (see Section 3.4). Combining the blockade of four currents exponentially increases the number of possibilities and simulations to be performed. The performance of the four arrhythmogenic biomarkers (including also T_{EAD}) depending on the affected currents considered is shown in Table S3. In general, it can be observed that when considering effects on less currents, the loss of accuracy is very small (less than 2%). In some cases, when simulating the effects on I_{Kr}, I_{NaL}, and I_{CaL}, the accuracy obtained is the same as when considering effects on the seven currents. On the other hand, considering that drugs have effects on I_{Kr}, I_{NaL}, and I_{CaL} provides better results than considering I_{Kr}, I_{Ks}, and I_{CaL}. This is consistent with the sensitivity analysis, since I_{NaL} has a greater influence than I_{Ks}.

With the new biomarker values, two more decision-tree-based classifiers were built. In addition, we built a third classifier that combined as input biomarkers calculated in both ways. That means, for example, that two different T_x values are considered in the tree, one calculated considering effects on I_{Kr}, I_{CaL}, and I_{Ks} and another T_x calculated, taking into account drug effects on I_{Kr}, I_{CaL}, and I_{NaL}. In Table 2, we can see how the classification performance changes depending on the currents considered to calculate the biomarkers. As expected,

https://dx.doi.org/10.1021/acs.jcim.0c00201
J. Chem. Inf. Model. 2020, 60, 5172−5187

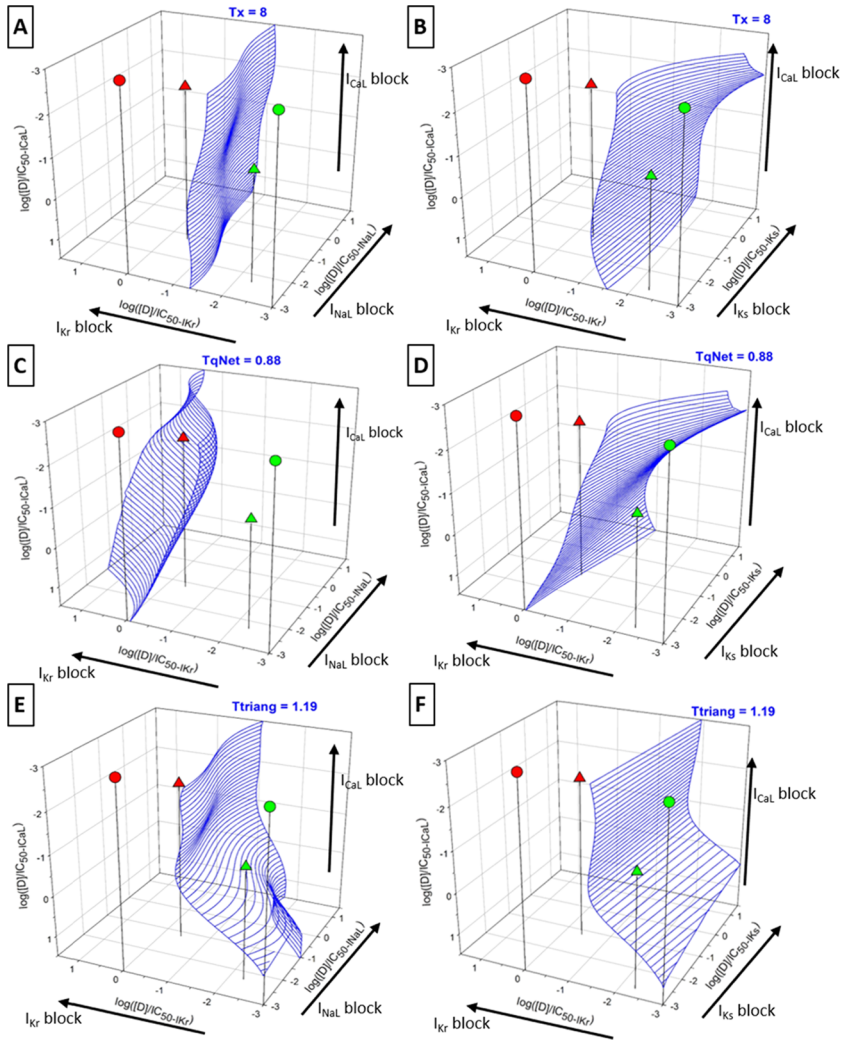

Figure 6. Precomputed matrices for the following arrhythmogenic indices: T_x (A and B), T_{qNet} (C and D), and T_{triang} (E and F). As an example of their usage, four drugs (two TdP+ and two TdP−) have been represented in each matrix: ibutilide (red circle), disopyramide (red triangle), loratadine (green circle), and diltiazem (green triangle). The axis represents the logarithm of the ratio of the drug concentration to the IC_{50} of each channel ($\log([D]/IC_{50})$). (A and B) Three-dimensional (3D) representation of the surface (blue striped) corresponding to $T_x = 8$. Torsadogenic drugs are on the left of this surface and safe drugs stay on the right of the surface. (C and D) 3D representation of the surface (blue striped) corresponding to $T_{qNet} = 0.88$. Again, torsadogenic drugs are on the left of this surface. (E and F) 3D representation of the surface (red striped) corresponding to $T_{triang} = 1.19$. Torsadogenic drugs are on the left of this surface, where blockades are higher.

when only the effects on I_{Kr}, I_{CaL}, and I_{Ks} or on I_{Kr}, I_{CaL}, and I_{NaL} were considered the accuracy of the classifier decreased, as all of the available information was not used. However, this loss of accuracy was remarkably very low. In fact, the accuracy of the classifier that uses biomarkers calculated taking into account drug effects on I_{Kr}, I_{CaL}, and I_{NaL} was only 0.9% lower than the accuracy of the classifier that takes into account the seven CiPA currents. The accuracy of the classifier when taking into account the effects on I_{Kr}, I_{CaL}, and I_{Ks} decreased by 1.8%. What is more surprising is that when combining biomarkers obtained in both ways (ones considering I_{Kr}, I_{CaL} and I_{Ks}, and others considering I_{Kr}, I_{CaL}, and I_{NaL}), the same level of accuracy that when considering the seven currents was achieved. In this case, the false negatives were the same, while the false positives were two class 3 drugs (fluvoxamine and ranolazine) and one class 4 compound (verapamil).

The performance of the classifiers depending on the biomarkers used as inputs is summarized in the Supporting information, Table S4. It can be observed that the maximum accuracy was obtained when considering the four biomarkers (T_x, T_{qNet}, T_{triang}, and T_{EAD}) to build the classifier (95.4%). However, the difference in performance when not considering T_{EAD} in the classifier is that just one more drug was misclassified (94.5% accuracy). In addition, in this case, out of the three false negatives, only one belongs to the class 1 of CredibleMeds (known risk of TdP), while when including T_{EAD} into the classifier, the two false negatives are two class 1 drugs. For this reason, and because T_{EAD} is a complex and computationally expensive biomarker, which, as shown in Section 3.1, has low predictive power as an individual predictor, T_{EAD} was not included in the preparation of the ready-to-use tool (see Section 3.4 for more details). For the other combinations of biomarkers, it can be observed that the accuracy fell slightly. It should also be noted that considering the effect on only three currents (I_{Kr}, I_{CaL}, and I_{NaL} or I_{Kr}, I_{CaL}, and I_{Ks}) hardly affected the performance of the classifier. Furthermore, when combining biomarkers obtained in both ways (ones considering I_{Kr}, I_{CaL} and I_{Ks}, and others considering

https://dx.doi.org/10.1021/acs.jcim.0c00201
J. Chem. Inf. Model. 2020, 60, 5172−5187

I_{Kr}, I_{CaL}, and I_{NaL}), the same level of accuracy that when considering the seven currents was achieved.

3.4. Precomputed Arrhythmogenic Indices. To facilitate the prediction of the potential proarrhythmic risk of a wide range of drugs without carrying out time-consuming simulations, T_x, T_{qNet}, and T_{triang} were precomputed for a large combination of I_{Kr}, I_{CaL}, I_{Ks}, and I_{NaL} block values (the most relevant currents according to the sensitivity analysis) and concentrations.

As mentioned above, combining biomarkers calculated taking into account the effects on I_{Kr}, I_{CaL}, and I_{Ks} with biomarkers calculated taking into account effects on I_{Kr}, I_{CaL}, and I_{NaL} improves the accuracy of a classifier. Indeed, its performance is very similar to that of the classifier that uses biomarkers calculated assuming effects on the seven CiPA currents.

For this reason, for each of the three biomarkers, we constructed two matrices, one in which the biomarker was calculated using a combination of drug concentrations over the IC_{50} of I_{Kr}, I_{CaL}, and I_{Ks} and another were the currents blocked were I_{Kr}, I_{CaL}, and I_{NaL}. Therefore, 492 536 simulations of drug effects on the isolated endocardial myocytes were run with a BCL of 1000 ms, varying the ratios of the drug concentration to the IC_{50} of each considered ion channel (I_{Kr}, I_{Ks}, and I_{CaL} in one case and I_{Kr}, I_{NaL}, and I_{CaL} in the other case). The logarithm of ratios of the drug concentration to the IC_{50} of each considered ion channel (I_{Kr}, I_{CaL}, I_{Ks}, and I_{NaL}) ranged from −3 to 1.5, with a 0.1 step increment. Note that if we had tried to calculate the biomarkers for all possible combinations of the four currents, the number of simulations would have amounted up to more than 8 000 000 simulations. In addition, the representation of the results would have been more complex.

Figure 6 shows the six matrices calculated. The matrix in panel A provides the T_x for a given combination of I_{Kr}, I_{CaL}, and I_{NaL} blockades. The stripped surface corresponds to the combination of blockades leading to $T_x = 8$. Panel B shows the T_x matrix depending on I_{Kr}, I_{CaL}, and I_{Ks} blockades. Panels C and D display the matrices for T_{qNet}. Panels E and F display the matrices for T_{triang}. The surfaces represented in each matrix correspond to the optimal cutoff point for each biomarker as an individual predictor ($T_{qNet} = 0.88$, $T_{triang} = 1.19$, see Section 3.1 for more details). These surfaces were represented only as a proof of concept, and different surfaces could have been represented. In each matrix, four drugs have been represented as an example: ibutilide (red circle), disopyramide (red triangle), loratadine (green circle), and diltiazem (green triangle).

The matrices can be used for two different purposes. On the one hand, they can be used to quickly predict whether an existing drug, for which all pharmacological data are known, is likely to produce TdP at its EFTPC. On the other hand, in the case of a drug candidate, they may be useful to help determine the TdP risk at a given concentration.

As an example, for a prediction based exclusively on T_x, we know that the threshold $T_x = 8$ is the one that best separates TdP+ drugs from TdP− drugs. Therefore, for a well-characterized drug, if we calculate the blockade of I_{Kr}, I_{CaL}, I_{NaL}, and I_{Ks} (i.e., $\log(\mathrm{EFTPC}/\mathrm{IC}_{50})$), we can use this matrix directly, without the need to run any simulation, to locate the drug in 3D plots like the ones represented in Figure 6A,B to know the associated T_x. We can see that torsadogenic compounds like ibutilide (red circle) and disopyramide (red triangle) fall to the right of this surface, meaning that their T_x is lower than 8. Conversely, nontorsadogenic compounds, like loratadine (green circle) and diltiazem (green triangle), fall to the right of the stripped surface. Therefore, their T_x is higher than 8. We can perform a similar approach for the other matrices, based on the cutoff value for each biomarker, so that we can observe that arrhythmogenic drugs are at one side of the surface and safe drugs at the opposite. More accurate predictions can be made using the evaluations of the decision-tree based classifier and combining the different matrices.

In the case of new compounds, as the EFTPC is unknown, these matrices can be used to find an estimation of the maximum safe concentration. For this purpose, an initial estimation of the maximum concentration has to be provided instead of the EFTPC, together with the IC_{50}s. For these values, the precomputed matrices will provide a set of indices. They can be compared to the cutoff point of each of the decision trees of the classifiers to obtain a set of conditions that must be accomplished to classify the drug as a safe compound. Then, if a certain biomarker, for example, T_x, does not accomplish the conditions because it is lower, the concentration should be decreased. On the contrary, if the T_x index is higher than the decision stated by the classifier, that means that the maximum safe concentration could be higher. If instead of T_x, a different index is considered, the procedure would be similar: increase or decrease the concentration to meet the conditions. Thus, to find a maximum safe concentration, the process must be repeated for several concentrations until the biomarkers are as near as possible to the cutoff point.

Matrices are available online on the public repository of the Polytechnic University of Valencia (RIUNET, https://riunet.upv.es/handle/10251/136919). Another advantage of these matrices is that by having the value of biomarkers available for a wide variety of drugs, new classification strategies can be proposed.

4. DISCUSSION

4.1. Main Findings. In this work, we present a new classifier for the evaluation of drug-induced torsadogenic risk during early stages based on three *in silico* biomarkers: T_x, T_{qNet}, and T_{triang}. Our main findings are (i) any of these arrhythmogenic indices, which collect the influence of relevant factors on the development of TdP, perform better than the current preclinical surrogate marker of TdP risk (hERG IC_{50}). (ii) When combining these arrhythmogenic indices into a classifier, the quality of the classification improves, showing better accuracy. The resulting accuracy of the binary classifier is 94.5%, misclassifying only six drugs out of 109. Misclassifications using the hERG block criterion were 23 (an accuracy of 78.9%). It should be noted that our classifiers were developed using 109 drugs and effects on seven ionic currents, being, to the best of our knowledge, one of the largest sets of drugs used in arrhythmogenic risk assessment. (iii) Considering drug effects on just four currents (I_{Kr}, I_{CaL}, I_{NaL}, and I_{Ks}), the ones with a greater impact on the biomarkers according to the sensitivity analysis, TdP risk classification can be as accurate as when taking into account the blockade of the seven currents of the CiPA initiative. This may allow experiments to be carried out, focusing on those most important currents, accelerating the drug development process and saving significant costs. (iv) Finally, this study also provides a ready-to-use tool available online based on more than 450 000 simulations of the electrophysiological activity of

https://dx.doi.org/10.1021/acs.jcim.0c00201
J. Chem. Inf. Model. 2020, 60, 5172−5187

ventricular cells. This tool consists of six matrices that contain the value of the three biomarkers for a wide range of I_{Kr}, I_{CaL}, I_{NaL}, and I_{Ks} blockades. This allows a quick assessment of the cardiotoxicity of existing drugs and helps in predicting the maximum safe free plasma concentration of new drugs that prevents TdP appearance.

4.2. Arrhythmogenic Indices. TdP risk-assessment methodologies based exclusively on the hERG block show low performance.[6,10,34] Indeed, when applying the pIC_{50} hERG test (TdP+: pIC_{50} hERG >5.8) to the 109 compounds studied in this work, the resulting sensitivity was 65% (18 false positives), the specificity was 91% (five false negatives), and the accuracy was 78.9%. This is in close agreement with previous studies[10,17,35] proposing classifications based on the hERG block that achieved accuracies around 70−80%. In 2003, Redfern et al.[36] proposed the ratio of the hERG IC_{50} over the maximum EFTPC as an improvement over the hERG IC_{50} index. They observed that a safety factor of 30 could provide a good torsadogenic risk prediction for 52 drugs. This metric has also been used in other studies as a current state-of-the-art measure.[16] In this study, in close agreement with Redfern et al.,[36] the cutoff point obtained for hERG IC_{50}/EFTPC was 39 and also showed better performance than simply hERG IC_{50}. Nevertheless, in comparison, all of the *in silico* biomarkers proposed in this study (with the exception of T_{EAD}) presented a higher performance, reducing the number of misclassified drugs.

The classification based on the analysis of EADs, which performed similar to pIC_{50} hERG, was not as predictive as the other *in silico* indices. Parikh et al.[26] also studied an EAD metric and observed a poor performance compared to other metrics, such as qNet. The reasons for the poor performance of the EAD biomarker might include inaccurate development of EADs in the used ionic model, as EADs are highly dependent on the ventricular cardiomyocyte model, or the need to test EADs on coupled cells/tissue models.[26] The influence of the model on the development of EADs can be highlighted in Passini et al.[13] In their work, they built a population of models by modifying some conductances of the O'Hara model within a physiological range. This way, they could cover a wider biological variability than just with a single AP and thus EADs obtained good accuracy as a biomarker for TdP risk. Another problem related to the O'Hara's model, which can explain the poor performance of EADs as a biomarker, is that it does not reproduce well the negative inotropic effect observed experimentally when simultaneously blocking I_{Na} and I_{NaL} Recently, Tomek et al.[37] published a model aiming to better reproduce this inotropic effect. Using the Tomek et al. model or other AP models will obviously result in the different performance of EADs as biomarkers (and also the performance of the other biomarkers), but this does not reduce the validity of the results presented in this work.

In a previous work,[10] we showed that the prediction of TdP risk could be improved with the T_x index. In that study, T_x was calculated taking into account the effects of drugs on I_{Kr}, I_{Ks}, and I_{CaL} and when applied to 84 compounds, it exhibited an accuracy of 87%. Here, considering drug effects on four currents to calculate T_x and applying this test to more drugs (109 drugs), the resulting accuracy was 89.9%. The threshold was the same in both works (T_x < 8 for TdP+ compounds). Therefore, this demonstrates that T_x is a robust and effective biomarker that can successfully be used for TdP risk evaluation.

As in previous recent studies,[5,15,26] T_{qNet} provided the most accurate proarrhythmic prediction among the four biomarkers. It should be said that Dutta et al.[15] correctly classified 100% using the qNet metric, but the data set studied was composed only the 12 CiPA training drugs. Here, when evaluating it with a larger set of drugs, its performance decreases. This is in accordance with Li et al.[5] results, where it is shown that qNet performance also decreases when considering the total 28 CiPA compounds. Note that T_{qNet} and qNet at 10×EFTPC perform equally, as T_{qNet} is qNet divided by a constant (qNet at control conditions). The advantage of using T_{qNet} is that it is a relative measure, which makes it independent of the model used. We chose 10×EFTPC because it is a concentration that produces significant drug effects without being an excessively high concentration. T_{triang} is also a relative metric that quantifies changes with respect to control conditions, which is an advantage with respect to triangulation. To the best of our knowledge, T_{triang} has not been used previously as an *in silico* classifier; however, it shows a performance very similar to that of previous TdP risk classification studies. Mirams et al.[8] assessed the performance of the prediction of the thorough QT assay in 34 drugs, obtaining 88% accuracy, 71% sensitivity, and 100% specificity. Lancaster and Sobie[12] have also evaluated arrhythmia risk combining multichannel block simulation of 68 drugs with statistical analysis and machine-learning techniques, achieving 89.5% accuracy, 95.9% sensitivity, and 81.1% specificity. Kramer et al.[17] observed that the TdP risk prediction provided by the comparison of the blocking potencies between I_{Kr} and I_{CaL} was drastically better than the prediction obtained by the hERG assay in 55 drugs (90.9% accuracy, 96.9% sensitivity, and 86.2% specificity). Parikh et al.[24] proposed a novel classifier that combined direct features (IC_{60} hERG) and 13 derived features. It provided an accuracy of 83% when tested in a merged data set of 197 drugs (some drugs were repeated as they were simulated using different drug models). Passini et al.[38] achieved an accuracy of 90% evaluating TdP risk of 40 drugs by measuring the shortening of the electromechanical window and repolarizations abnormalities. Li et al.[5] showed that their torsade metric score, which is the qNet value averaged across $1-4 \times C_{max}$ taking into account drug effects on the currents I_{Kr}, I_{Na}, I_{NaL}, and I_{CaL}, could successfully predict the TdP risk of the 16 CiPA compounds, outperforming other *in silico* metrics such as APD90 or APD50 and diastolic Ca^{2+} concentration. Recently, Zhou et al.[39] used the TdP risk score, a metric that summarizes repolarization abnormalities among a population of cardiomyocytes, to study how different prediction outcomes were, depending on the input data (IC_{50} and the Hill coefficient). This metric demonstrated good performance, showing an accuracy superior than to 80% on two different drug data sets.

In addition, we showed that combining T_x, T_{qNet}, and T_{triang} in a binary classifier based on decision trees improves the accuracy of risk classification up to 94.5%. In addition, this level of performance can be achieved simulating effects only on I_{Kr}, I_{CaL}, I_{NaL}, and I_{Ks}, which are the currents with a greater impact on the arrhythmogenic indices according to the sensitivity analysis. These results are comparable or even better than other more complex systems that perform 3D simulations and comparable to *in vitro* experiments with cells or whole hearts. Okada et al.[14] simulated a total of 9075 electrocardiograms using a 3D whole-ventricle model for a combination of blocks of I_{Kr}, I_{Na}, I_{NaL}, I_{CaL}, and I_{Ks}. Using this system, they evaluated 13 drugs, successfully classifying 92%.

https://dx.doi.org/10.1021/acs.jcim.0c00201
J. Chem. Inf. Model. 2020, 60, 5172−5187

Lawrence et al.[40] used the rabbit isolated Langerdorff heart model to investigate the torsadogenic risk of 64 compounds with an accuracy of 75%. Ando et al.[41] recorded extracellular field potentials from human iPSC-derived cardiomyocytes to evaluate 60 drugs achieving a sensitivity of 81%, a specificity of 87%, and an accuracy of 83%.

We observed that there was a group of drugs that was misclassified in all or in almost all cases. This indicates that the model is not reproducing some drug effects correctly or that experimental data might have some bias. There are pharmacological aspects that were not considered in this study mainly due to a lack of information, such as effects of metabolites, accumulation of the compound in the myocardium, channel trafficking inhibition, among others (all of them not included in the electrophysiological model used). It has been demonstrated that donepezil increased TdP incidence not only by I_{Kr} block but also by the I_{Kr} trafficking inhibition.[42,43] Ritonavir and saquinavir, which are misclassified with the binary classifier, are known to inhibit major isoforms of cytochrome P450,[14] which metabolize many drugs, including torsadogenic drugs such bepridil or quinidine. Thus, rather than its arrhythmogenic capacity per se, its torsadogenicity is due to the increase in the amount of other dangerous drugs. Cilostazol inhibits phosphodiesterase 3 (PDE3), which causes an increase in intracellular cAMP, Ca^{2+} dynamic unbalance, and precipitation of EADs.[44] Fluvoxamine has been classified as a class 3 compound by CredibleMeds, so here it was considered as TdP−. However, some clinical studies[45,46] reported that fluvoxamine, at therapeutic doses, increases the risk of TdP induction. These authors recommend that patients on fluvoxamine treatment should be monitored closely for QT/QTc interval prolongation with serial ECG. For propafenone, something similar occurred: it was classified as a class 3 compound by CredibleMeds, but different studies[47,48] alert about its TdP risk. In addition, in the American College of Cardiology website, there is a black box warning stating: "potentially fatal ventricular arrhythmias may occur with/without QT prolongation and can lead to torsade de pointes". It is worth noting that for cibenzoline only two studies reporting an IC_{50} I_{Kr} value were found and the difference between these two values was more than an order of magnitude. Therefore, its effect on I_{Kr} might have been overestimated and therefore resulted in a false positive. In the case of verapamil, the reason of its misclassification could be an overestimation of IC_{50} I_{Kr} that produces such a blockade that cannot be counteracted by the I_{CaL} blockade to avoid prolongation of the AP.[19] Therefore, it seems that this mechanism would require fine-tuning of the I_{CaL} and I_{Kr} ratios.

Other authors have predicted the cardiac safety of torsadogenic drugs simulating drug effects in isolated endocardial cells of different species such as guinea pigs,[9] dogs, or rabbits. Beattie et al.[49] predicted the experimental results of the rabbit left ventricular wedge assay using *in silico* simulations of the QT prolongation of the rabbit left ventricular wedge assay (78% accuracy). We chose a modified version of the O'Hara et al.[18] human ventricular AP model for our simulations instead of models of other species to obtain more accurate predictions of drug effects in humans.[50] In fact, compared to human cardiomyocytes, guinea pig cardiomyocytes showed a lack of transient outward current (I_{to}) and a large I_{Ks} and rabbit cardiomyocytes presented a small slow delayed rectifier current (I_{Ks}) and TdP predisposition.[51] In the human ventricular AP model, we decided not to introduce the dynamic-hERG model,[52] which is the most updated version recommended by the CiPA initiative for prediction of TdP, because many drugs do not have the experimental data necessary to model their effect and significantly increases the computational cost without providing significant benefits for the simulation of the effects of many drugs.[19]

4.3. Sensitivity Analysis. Our sensitivity analysis of the virtual population of drugs identified critical ionic currents for the variability of the different arrhythmogenic biomarkers studied for TdP risk assessment. The sensitivity analysis was performed using three different methods (see Section 2.4), and the three methods identify the same currents as the most influential: I_{Kr}, I_{CaL}, I_{NaL}, and I_{Ks}.

In agreement with previous studies,[8,18,20,23,26,53] I_{Kr} inhibition and I_{NaL} and I_{CaL} enhancement prolong APD_{90} and increase triangulation. Parikh et al.[26] also found that T_{qNet_mod} was more sensitive to changes in I_{NaL} and I_{Kr}. This relevant role of I_{NaL} is in agreement with experimental results, indicating that drug-induced enhancement of I_{NaL} can result in increased TdP risk in the absence of the hERG block.[54,55] Furthermore, according to Parikh et al.,[26] we have seen that some ion channels that are thought to be important for drug-induced TdP risk assessment and measured experimentally via *in-vitro* ion-channel screening[56] showed a minor influence on the arrhythmogenic biomarkers. For example, the block of I_{to} had no influence on most of the metrics. These facts suggest that the experimental and *in silico* study of the effects of drugs on I_{Kr}, I_{NaL}, I_{CaL}, and I_{Ks} is more relevant than drug effects on I_{to}, I_{Na} or I_{K1} for the assessment of TdP risk. Uncertainties in the input parameters that are highly influential, such as pharmacological data of the effects on the hERG channel, result in lower confidence in the predicted TdP risk, while errors in estimating less influential model parameters are better tolerated by risk measurements. Thus, Costabal et al.[53] showed that the variability in the I_{Kr} block, the current with the greatest sensitivity here, was primarily responsible for the uncertainty of QT interval simulations. In this work, we have demonstrated that using data from I_{Kr}, I_{NaL}, I_{CaL}, and I_{Ks}, torsadogenicity prediction is very similar to the results obtained using the seven currents. Recently, Zhou et al.[39] claimed that the minimum set of ion channels needed to correctly assess TdP risk were I_{Kr}, I_{CaL}, and I_{Na}. One of the reasons that explain this discrepancy between the minimum set of currents may be that they only compared the prediction results when considering drug effects on the seven currents, four (I_{Na}, I_{NaL}, I_{Kr}, and I_{CaL}), three (I_{Na}, I_{Kr} and I_{CaL}), or one (I_{Kr}). Perhaps, if other combinations of currents had been tested, another set of currents would have also led to similar accuracy. In addition, experimental data on I_{NaL} IC_{50} are only available for 25 of the 85 drugs studied. There are also very few data available for IC_{50} I_{Ks}. However, their results agree with this study in that not all seven CiPA currents are necessary. Simulating drug effects on a lower number of currents can achieve very accurate predictions. Furthermore, in both studies, I_{Kr} and I_{CaL} are a fundamental requirement. Our study suggests that they should be complemented with I_{NaL} or I_{Ks} to improve the accuracy of the prediction.

4.4. Limitations of the Study. One of the strengths of this work is the use of a large drug dataset including information of seven ionic currents. However, the IC_{50} values of some ionic currents of certain drugs were absent in the literature or public repositories. For example, to the best of our knowledge, the only work that provides information about I_{NaL}

https://dx.doi.org/10.1021/acs.jcim.0c00201
J. Chem. Inf. Model. 2020, 60, 5172−5187

block potency is Crumb et al.,[56] and they only studied 30 compounds. As illustrated above, I_{NaL} is one of the most influential currents in TdP prediction, so having more information about the blocking of I_{NaL} could improve the performance of the classifiers proposed here. For I_{to} and I_{K1}, available IC_{50} data were also scarce. In these cases, similar to previous studies,[8,10,24] no block of these channels was assumed. In addition, the IC_{50} and EFTPC values were consulted in heterogeneous sources, which suggests that the experimental conditions were very diverse and therefore there is also great variability in the collected data. In fact, some authors[57] have found that the IC_{50} values of I_{Kr} can vary by 1 or 2 orders of magnitude between different studies. Due to the lack of standard protocols, dealing with multiple IC_{50} for a given compound is a challenging task, which can be addressed in different ways. We reduced sources of variability by obtaining data from mammalian tissue registers when available and always avoiding data extracted from Xenopus oocytes. In addition, when multiple IC_{50} values were available for a given drug, the median value was calculated. As recently demonstrated by Zhou et al.,[39] for compounds with multiple ion-channel potencies, variations in the IC_{50} value can lead to different *in silico* predictions. In this work, they studied prediction divergencies using two different data sets: Crumb's data set[56] and Kramer's data set.[17] They showed that the accuracy when using Crumb's values was slightly higher than when using Kramer's values. Here, we considered that the published data represented a distribution of values affected by a random error and the variability due to the experimental conditions. Then, the most representative value considering variability was the median as it is a robust estimator of the central tendency of a data set, less sensitive to extreme values than the average. Further studies on uncertainty quantification will help us to better understand model's tolerability of input variability. In addition, standardization of experimental protocols, with well-defined environmental conditions, could help increase the model prediction accuracy, as it has been highlighted by Li et al.[5] Recently, Gomis-Tena et al.[58] showed that for some drugs, even maintaining the same experimental conditions, IC_{50} value may vary, depending on the voltage-clamp protocol used, and proposed the adoption of a three-protocol IC_{50} assay to measure the potency to block hERG.

Here, similar to other studies,[5] we used the cross-validation method to validate TdP risk predictions, where for each iteration some drugs are used as the training set and others as the validation set. Recently, Li et al.[59] proposed a new training-validation strategy to validate TdP prediction models. They proposed that the models should be validated by an external set of drugs ("hidden" validation group), where experimental data are not even collected for validation drugs during the model training stage. In this sense, this strategy could be taken into account in the future.

On the other hand, we simulated drug effects using the simple pore block model, which assumes that the union between a drug and a channel can occur in any channel conformation and that the channel activity kinetics remain unchanged after binding.[60] This may be too simplistic and may not capture adequately complex pharmacokinetic or pharmacodynamic effects. For example, drug binding kinetics, which were not considered in this work, have been related to increased susceptibility to acquired long QT syndrome in the presence of hERG channel kinetic abnormalities.[52] Simulations of hERG drug binding kinetics could have been modeled through the recently introduced dynamic-hERG model.[61,62] However, experimental parameters needed to simulate drug effects are scarce because they are measured using complex experimental protocols.[24] This dynamic-hERG model needs five more parameters to simulate the effects of a given drug, and it has been proved that parameters such as V_{half} and K_u contribute relatively little to the variation of qNet, APD_{90}, and $[Ca^{2+}]_i$ peak.[19] In addition, using these models does not bring benefits for many drugs as there are no significant changes in the simulations.[63]

Our simulations do not consider other pharmacological aspects such as drug−drug interactions, effects of active metabolites, accumulation of drugs in cardiac tissues, effects on the autonomic nervous system, protein binding alterations, etc. Drug−drug interactions play a role in torsadogenic induction of drugs such as clozapine and risperidone[64] or domperidone.[65] The incorporation of such aspects could have enriched the results of this study. Unfortunately, further experimental studies are needed to provide the data for all of the compounds considered here to allow the simulation of these phenomena. Nevertheless, it can be said that the levels of accuracy obtained in this work suggest that the most relevant biophysical processes contributing to the induction of TdP have been correctly represented.

Another limitation of this work is that the results of the classification depend largely on the information taken as reference. Here, drugs were classified according to the CredibleMeds database, which feeds from clinical data and is well recognized by the scientific community. We have considered class 3 (conditional risk drugs) as TdP−, since we have focused on the individual pharmacological effects (not interactions) on healthy cells and therefore we considered that these special conditions did not take place and these drugs had little probability of causing TdP. In addition, we have considered the worst possible scenario, that is, the highest EFTPC of those published. However, specific conditions such as overdose can increase the arrhythmogenic potential of these drugs. In this sense, we tested how the prediction of the TdP risk classifier for class 3 compounds changed under therapeutic doses or under overdose conditions (10×EFTPC). As previously shown (Table 2), at 1×EFTPC, there is just one class 3 drug (fluvoxamine) that is predicted by the decision-tree-based classifier as TdP+, while in overdose conditions, seven out of these 13 drugs increased their torsadogenicity and were considered as TdP+: fluvoxamine and diphenhydramine, metronidazole, paroxetine, quetiapine, solifenacin, and voriconazole. Furthermore, some other drugs may change their level of proarryhtmicity depending on the database. For example, drugs such as astemizole, chlorpromazine, cisapride, clarithromycin, domperidone, droperidol, terfenadine, pimozide, or ondansetron, which are considered as high-risk drugs according to CredibleMeds, belong to the group of intermediate-risk drugs in the CiPA developing set. Ranolazine and tamoxifen are intermediate risk drugs according to CredibleMeds, but they are low risk accorging to the CiPA set. In fact, Wiśniowska and Polak[65] provided a large number of drugs with contradicting classification among different databases. Thus, different categorizations can lead to different accuracies and performances of the TdP risk classifier. This highlights the need for a standardized TdP risk drug classification to obtain a wide database (ground truth) that helps researchers to develop new tools for proarrhythmic risk prediction.

https://dx.doi.org/10.1021/acs.jcim.0c00201
J. Chem. Inf. Model. 2020, 60, 5172−5187

5. CONCLUSIONS

In this work, we describe a new *in silico* tool to study the effects of a drug on the electrophysiological properties of a cardiomyocyte and thus predict its proarrhythmic risk. Our results highlight that *in silico* simulations considering the EFTPC and the effects on ionic currents improve the prediction of cardiotoxicity, in addition to the well-proven influence of hERG IC_{50} (current TdP risk biomarker according to S7B ICH guidelines) on the likelihood of TdP. We also show that it is not necessary to simulate the drug effects on the main seven ionic currents proposed by CiPA to have a good prediction of the proarrhythmicity of a compound. With experimental data of four currents (I_{Kr}, I_{CaL}, I_{NaL}, and I_{Ks}, which are the currents with a greater impact on the arrhythmogenic indices according to the sensitivity analysis), TdP prediction can be significantly accurate. In addition, we provide a ready-to-use tool which can be used to estimate the maximum safe free plasma concentration in the different phases of drug discovery or to quickly assess the proarrhythmicity of a drug with known EFTPC and IC_{50}s. We believe that the usage of such *in silico* tools as screening methods could be helpful to accelerate the development of new drugs and reduce the costs of cardiac safety screening in preclinical phases. In addition, this approach has the potential to lead to a major replacement of animal experiments in the early stages of drug development.

■ ASSOCIATED CONTENT

Supporting Information

The Supporting Information is available free of charge at https://pubs.acs.org/doi/10.1021/acs.jcim.0c00201.

> Equations of the activation (m_{ss}) and inactivation gates (h_{ss}, h_{ssp}, and j_{ss}) at the steady state of the rapid Na^+ current in the O'Hara et al. model and in the modified version. IC_{50} values (nM), Hill coefficients, and effective free therapeutic plasma concentration (EFTPC) (nM) used to simulated the 109 drugs studied in this work. Performance of the four arrhythmogenic biomarkers depending on the currents on which the effect of the drug is assumed: the seven CiPA currents; I_{Kr}, I_{CaL}, and I_{Ks}, or, I_{Kr}, I_{CaL}, and I_{NaL}. Performance of the classifiers depending on the biomarkers used as inputs. Results of the sensitivity analysis with the multiple linear regression method. Results of the sensitivity analysis applying the PLS method. Decision trees that constitute the binary TdP risk classifier based on T_x, T_{qNet}, and T_{triang} (PDF)

■ AUTHOR INFORMATION

Corresponding Author

Beatriz Trenor − *Centro de Investigación e Innovación en Bioingeniería (Ci2B), Universitat Politècnica de València, 46022 Valencia, Spain*; Phone: +34 963877007; Email: btrenor@eln.upv.es; Fax: 76086/67039

Authors

Jordi Llopis-Lorente − *Centro de Investigación e Innovación en Bioingeniería (Ci2B), Universitat Politècnica de València, 46022 Valencia, Spain*

Julio Gomis-Tena − *Centro de Investigación e Innovación en Bioingeniería (Ci2B), Universitat Politècnica de València, 46022 Valencia, Spain*

Jordi Cano − *Centro de Investigación e Innovación en Bioingeniería (Ci2B), Universitat Politècnica de València, 46022 Valencia, Spain*; orcid.org/0000-0001-9461-9848

Lucía Romero − *Centro de Investigación e Innovación en Bioingeniería (Ci2B), Universitat Politècnica de València, 46022 Valencia, Spain*

Javier Saiz − *Centro de Investigación e Innovación en Bioingeniería (Ci2B), Universitat Politècnica de València, 46022 Valencia, Spain*

Complete contact information is available at: https://pubs.acs.org/10.1021/acs.jcim.0c00201

Author Contributions

J.L.L. contributed to the design of the study, performed the simulations, analyzed the results, and wrote the first draft of the manuscript. J.G.-T. implemented the model in C++, built the matrices of the precomputed indices, and obtained the figures of the matrices. B.T. and J.S. contributed to the design of the study, analyzed the results, and supervised the project. All authors contributed to manuscript revision and read and approved the submitted version.

Funding

This work was partially supported by the Dirección general de Política Científica de la Generalitat Valenciana (PROMETEO/2020/043); by "Primeros Proyectos de Investigación" (PAID-06-18) from Vicerrectorado de Investigación, Innovación y Transferencia de la Universitat Politècnica de València (UPV), València, Spain; as well as from the "Plan Estatal de Investigación Científica y Técnica y de Innovación 2017−2020" from the Ministerio de Ciencia e Innovación y Universidades (PID2019-104356RB-C41/AEI/10.13039/501100011033). J.L.L. is being funded by the Ministerio de Ciencia, Innovación y Universidades for the "Formación de Profesorado Universitario" (Grant Reference: FPU18/01659).

Notes

The authors declare no competing financial interest.

T_x, T_{qNet}, and T_{triang} pre-computed matrices and Matlab functions used in this work are available free of charge at: https://riunet.upv.es/handle/10251/136919.

■ ACKNOWLEDGMENTS

The authors would like to immensely thank Dr. Manuel Pastor from the Research Programme on Biomedical Informatics (GRIB), at Universitat Pompeu Fabra (Barcelona, Spain), for his review of the manuscript and expert opinions and suggestions.

■ REFERENCES

(1) Li, M.; Ramos, L. G. Drug Induced QT Prolongation and Torsades de Pointes. *Pharmacol. Ther.* **2017**, *42*, 473−477.

(2) Gintant, G. A. Preclinical Torsades-de-Pointes Screens: Advantages and Limitations of Surrogate and Direct Approaches in Evaluating Proarrhythmic Risk. *Pharmacol. Ther.* **2008**, *119*, 199−209.

(3) Vicente, J.; Zusterzeel, R.; Johannesen, L.; Mason, J.; Sager, P.; Patel, V.; Matta, M. K.; Li, Z.; Liu, J.; Garnett, C.; Stockbridge, N.; Zineh, I.; Strauss, D. G. Mechanistic Model-Informed Proarrhythmic Risk Assessment of Drugs: Review of the "CiPA" Initiative and Design of a Prospective Clinical Validation Study. *Clin. Pharmacol. Ther.* **2018**, *103*, 54−66.

(4) Colatsky, T.; Fermini, B.; Gintant, G.; Pierson, J. B.; Sager, P.; Sekino, Y.; Strauss, D. G.; Stockbridge, N. The Comprehensive in Vitro Proarrhythmia Assay (CiPA) Initiative — Update on Progress. *J. Pharmacol. Toxicol. Methods* **2016**, *81*, 15−20.

(5) Li, Z.; Ridder, B. J.; Han, X.; Wu, W. W.; Sheng, J.; Tran, P. N.; Wu, M.; Randolph, A.; Johnstone, R. H.; Mirams, G. R.; Kuryshev, Y.; Kramer, J.; Wu, C.; Crumb, W. J.; Strauss, D. G. Assessment of an In Silico Mechanistic Model for Proarrhythmia Risk Prediction Under the CiPA Initiative. *Clin. Pharmacol. Ther.* **2019**, *105*, 466−475.
(6) Sager, P. T.; Gintant, G.; Turner, J. R.; Pettit, S.; Stockbridge, N. Rechanneling the Cardiac Proarrhythmia Safety Paradigm: A Meeting Report from the Cardiac Safety Research Consortium. *Am. Heart J.* **2014**, *167*, 292−300.
(7) Fermini, B.; Hancox, J. C.; Abi-Gerges, N.; Bridgland-Taylor, M.; Chaudhary, K. W.; Colatsky, T.; Correll, K.; Crumb, W.; Damiano, B.; Erdemli, G.; Gintant, G.; Imredy, J.; Koerner, J.; Kramer, J.; Levesque, P.; Li, Z.; Lindqvist, A.; Obejero-Paz, C. A.; Rampe, D.; Sawada, K.; Strauss, D. G.; Vanderberg, J. I. A New Perspective in the Field of Cardiac Safety Testing through the Comprehensive in Vitro Proarrhythmia Assay Paradigm. *J. Biomol. Screen.* **2016**, *21*, 1−11.
(8) Mirams, G. R.; Davies, M. R.; Brough, S. J.; Bridgland-Taylor, M. H.; Cui, Y.; Gavaghan, D. J.; Abi-Gerges, N. Prediction of Thorough QT Study Results Using Action Potential Simulations Based on Ion Channel Screens. *J. Pharmacol. Toxicol. Methods* **2014**, *70*, 246−254.
(9) Obiol-Pardo, C.; Gomis-Tena, J.; Sanz, F.; Saiz, J.; Pastor, M. A Multiscale Simulation System for the Prediction of Drug-Induced Cardiotoxicity. *J. Chem. Inf. Model.* **2011**, *51*, 483−492.
(10) Romero, L.; Cano, J.; Gomis-Tena, J.; Trenor, B.; Sanz, F.; Pastor, M.; Saiz, J. In Silico QT and APD Prolongation Assay for Early Screening of Drug-Induced Proarrhythmic Risk. *J. Chem. Inf. Model.* **2018**, *58*, 867−878.
(11) Trenor, B.; Gomis-Tena, J.; Cardona, K.; Romero, L.; Rajamani, S.; Belardinelli, L.; Giles, W. R.; Saiz, J. In Silico Assessment of Drug Safety in Human Heart Applied to Late Sodium Current Blockers. *Channels* **2013**, *7*, 249−262.
(12) Lancaster, M. C.; Sobie, E. A. Improved Prediction of Drug-Induced Torsades de Pointes Through Simulations of Dynamics and Machine Learning Algorithms. *Clin. Pharmacol. Ther.* **2016**, *100*, 371−379.
(13) Passini, E.; Britton, O. J.; Lu, H. R.; Rohrbacher, J.; Hermans, A. N.; Gallacher, D. J.; Greig, R. J. H.; Bueno-Orovio, A.; Rodriguez, B. Human in Silico Drug Trials Demonstrate Higher Accuracy than Animal Models in Predicting Clinical Pro-Arrhythmic Cardiotoxicity. *Front. Physiol.* **2017**, *8*, No. 668.
(14) Okada, J.; Yoshinaga, T.; Kurokawa, J.; Washio, T.; Furukawa, T.; Sawada, K.; Sugiura, S.; Hisada, T. Arrhythmic Hazard Map for a 3D Whole-Ventricle Model under Multiple Ion Channel Block. *Br. J. Pharmacol.* **2018**, *175*, 3435−3452.
(15) Dutta, S.; Chang, K. C.; Beattie, K. A.; Sheng, J.; Tran, P. N.; Wu, W. W.; Wu, M.; Strauss, D. G.; Colatsky, T.; Li, Z. Optimization of an in Silico Cardiac Cell Model for Proarrhythmia Risk Assessment. *Front. Physiol.* **2017**, *8*, No. 616.
(16) Mirams, G. R.; Cui, Y.; Sher, A.; Fink, M.; Cooper, J.; Heath, B. M.; McMahon, N. C.; Gavaghan, D. J.; Noble, D. Simulation of Multiple Ion Channel Block Provides Improved Early Prediction of Compounds' Clinical Torsadogenic Risk. *Cardiovasc. Res.* **2011**, *91*, 53−61.
(17) Kramer, J.; Obejero-Paz, C. A.; Myatt, G.; Kuryshev, Y. A.; Bruening-Wright, A.; Verducci, J. S.; Brown, A. M. MICE Models: Superior to the HERG Model in Predicting Torsade de Pointes. *Sci. Rep.* **2013**, *3*, No. 2100.
(18) O'Hara, T.; Virág, L.; Varró, A.; Rudy, Y. Simulation of the Undiseased Human Cardiac Ventricular Action Potential: Model Formulation and Experimental Validation. *PLoS Comput. Biol.* **2011**, *7*, No. e1002061.
(19) Britton, O. J.; Abi-Gerges, N.; Page, G.; Ghetti, A.; Miller, P. E.; Rodriguez, B. Quantitative Comparison of Effects of Dofetilide, Sotalol, Quinidine, and Verapamil between Human Ex Vivo Trabeculae and in Silico Ventricular Models Incorporating Inter-Individual Action Potential Variability. *Front. Physiol.* **2017**, *8*, No. 597.
(20) Passini, E.; Mincholé, A.; Coppini, R.; Cerbai, E.; Rodriguez, B.; Severi, S.; Bueno-Orovio, A. Mechanisms of Pro-Arrhythmic Abnormalities in Ventricular Repolarisation and Anti-Arrhythmic Therapies in Human Hypertrophic Cardiomyopathy. *J. Mol. Cell. Cardiol.* **2016**, *96*, 72−81.
(21) Cavero, I.; Guillon, J. M.; Ballet, V.; Clements, M.; Gerbeau, J. F.; Holzgrefe, H. Comprehensive in Vitro Proarrhythmia Assay (CiPA): Pending Issues for Successful Validation and Implementation. *J. Pharmacol. Toxicol. Methods* **2016**, *81*, 21−36.
(22) Dutta, S.; Strauss, D.; Colatsky, T.; Li, Z. In *Optimization of an In Silico Cardiac Cell Model for Proarrhythmia Risk Assessment*, 2016 Computing in Cardiology Conference (CinC); 2016; pp 869−872.
(23) Mora, M. T.; Ferrero, J. M.; Romero, L.; Trenor, B. Sensitivity Analysis Revealing the Effect of Modulating Ionic Mechanisms on Calcium Dynamics in Simulated Human Heart Failure. *PLoS One* **2017**, *12*, No. e0187739.
(24) Parikh, J.; Gurev, V.; Rice, J. J. Novel Two-Step Classifier for Torsades de Pointes Risk Stratification from Direct Features. *Front. Pharmacol.* **2017**, *8*, No. 816.
(25) Woosley, R.; Romero, K.; Heise, W. *Risk Categories for Drugs that Prolong QT & Induce Torsade de Pointes (TdP)*; AZCERT, Inc.: Oro Valley, AZ, 2019. https://www.crediblemeds.org/ (accessed March 9, 2020).
(26) Parikh, J.; di Achille, P.; Kozloski, J.; Gurev, V. Global Sensitivity Analysis of Ventricular Myocyte Model-Derived Metrics for Proarrhythmic Risk Assessment. *Front. Pharmacol.* **2019**, *10*, No. 1054.
(27) Varró, A.; Baczkó, I. Cardiac Ventricular Repolarization Reserve: A Principle for Understanding Drug-Related Proarrhythmic Risk. *Br. J. Pharmacol.* **2011**, *164*, 14−36.
(28) Antzelevitch, C. Ionic, Molecular, and Cellular Bases of QT-Interval Prolongation and Torsade de Pointes. *EP Europace* **2007**, *9*, iv4−iv15.
(29) Viswanathan, P. C.; Rudy, Y. Pause Induced Early Afterdepolarizations in the Long QT Syndrome: A Simulation Study. *Cardiovasc. Res.* **1999**, *42*, 530−542.
(30) Britton, O. J.; Bueno-Orovio, A.; van Ammel, K.; Lu, H. R.; Towart, R.; Gallacher, D. J.; Rodriguez, B. Experimentally Calibrated Population of Models Predicts and Explains Intersubject Variability in Cardiac Cellular Electrophysiology. *Proc. Natl. Acad. Sci. U.S.A.* **2013**, *110*, e2098−e2105.
(31) Sobie, E. A. Parameter Sensitivity Analysis in Electrophysiological Models Using Multivariable Regression. *Biophys. J.* **2009**, *96*, 1264−1274.
(32) Hair, J. F.; Black, B.; Babin, B.; Anderson, R. E. *Multivariate Data Analysis*, 7th ed.; Pearson Prentice Hall: Upper Saddle River, NJ, 2010.
(33) James, G. *Majority Vote Classifiers: Theory and Applications*; Stanford University: United States, 1998.
(34) Hoffmann, P.; Warner, B. Are HERG Channel Inhibition and QT Interval Prolongation All There Is in Drug-Induced Torsadogenesis? A Review of Emerging Trends. *J. Pharmacol. Toxicol. Methods* **2006**, *53*, 87−105.
(35) Cantilena, L. R., Jr.; Koerner, J.; Temple, R.; Throckmorton, D. FDA Evaluation of Cardiac Repolarization Data for 19 Drugs and Drug Candidates. *Clin. Pharmacol. Ther.* **2006**, *79*, P29.
(36) Redfern, W. S.; Carlsson, L.; Davis, A. S.; Lynch, W. G.; MacKenzie, I.; Palethorpe, S.; Siegl, P. K. S.; Strang, I.; Sullivan, A. T.; Wallis, R.; Camm, A. J.; Hammond, T. G. Relationships between Preclinical Cardiac Electrophysiology, Clinical QT Interval Prolongation and Torsade de Pointes for a Broad Range of Drugs: Evidence for a Provisional Safety Margin in Drug Development. *Cardiovasc. Res.* **2003**, *58*, 32−45.
(37) Tomek, J.; Bueno-Orovio, A.; Passini, E.; Zhou, X.; Minchole, A.; Britton, O.; Bartolucci, C.; Severi, S.; Shrier, A.; Virag, L.; Varro, A.; Rodriguez, B. Development, Calibration, and Validation of a Novel Human Ventricular Myocyte Model in Health, Disease, and Drug Block. *eLife* **2019**, *8*, No. e48890.
(38) Passini, E.; Trovato, C.; Morissette, P.; Sannajust, F.; Bueno-Orovio, A.; Rodriguez, B. Drug-Induced Shortening of the Electromechanical Window Is an Effective Biomarker for in Silico Prediction

of Clinical Risk of Arrhythmias. *Br. J. Pharmacol.* **2019**, *176*, 3819−3833.
(39) Zhou, X.; Qu, Y.; Passini, E.; Bueno-Orovio, A.; Liu, Y.; Vargas, H. M.; Rodriguez, B. Blinded In Silico Drug Trial Reveals the Minimum Set of Ion Channels for Torsades de Pointes Risk Assessment. *Front. Pharmacol.* **2020**, *10*, No. 1643.
(40) Lawrence, C. L.; Bridgland-Taylor, M. H.; Pollard, C. E.; Hammond, T. G.; Valentin, J. P. A Rabbit Langendorff Heart Proarrhythmia Model: Predictive Value for Clinical Identification of Torsades de Pointes. *Br. J. Pharmacol.* **2006**, *149*, 845−860.
(41) Ando, H.; Yoshinaga, T.; Yamamoto, W.; Asakura, K.; Uda, T.; Taniguchi, T.; Ojima, A.; Shinkyo, R.; Kikuchi, K.; Osada, T.; Hayashi, S.; Kasai, C.; Miyamoto, N.; Tashibu, H.; Yamakazi, D.; Sugiyama, A.; Kanda, Y.; Sawada, K.; Sekino, Y. A New Paradigm for Drug-Induced Torsadogenic Risk Assessment Using Human IPS Cell-Derived Cardiomyocytes. *J. Pharmacol. Toxicol. Methods* **2017**, *84*, 111−127.
(42) Cubeddu, L. Drug-Induced Inhibition and Trafficking Disruption of Ion Channels: Pathogenesis of QT Abnormalities and Drug-Induced Fatal Arrhythmias. *Curr. Cardiol. Rev.* **2016**, *12*, 141−154.
(43) Nogawa, H.; Kawai, T. HERG Trafficking Inhibition in Drug-Induced Lethal Cardiac Arrhythmia. *Eur. J. Pharmacol.* **2014**, *741*, 336−339.
(44) Kanlop, N.; Chattipakorn, S.; Chattipakorn, N. Effects of Cilostazol in the Heart. *J. Cardiovasc. Med.* **2011**, *12*, 88−95.
(45) Morosin, M.; Dametto, E.; del Bianco, F.; Brieda, M.; Nicolosi, G. L. An Unusual Etiology of Torsade de Pointes-Induced Syncope. *Arch. Med. Sci.* **2017**, *13*, 686−688.
(46) Nia, A. M.; Dahlem, K. M.; Gassanov, N.; Hungerbühler, H.; Fuhr, U.; Er, F. Clinical Impact of Fluvoxamine-Mediated Long QTU Syndrome. *Eur. J. Clin. Pharmacol.* **2012**, *68*, 109−111.
(47) Hii, J. T. Y.; Wyse, D. G.; Gillis, A. M.; Cohen, J. M.; Mitchell, L. B. Propafenone-Induced Torsade de Pointes: Cross-Reactivity with Quinidine. *Pacing Clin. Electrophysiol.* **1991**, *14*, 1568−1570.
(48) Wenzel-Seifert, K.; Wittmann, M.; Haen, E. QTc Prolongation by Psychotropic Drugs and the Risk of Torsade de Pointes. *Dtsch. Arztebl. Int.* **2011**, *108*, 687−693.
(49) Beattie, K. A.; Luscombe, C.; Williams, G.; Munoz-Muriedas, J.; Gavaghan, D. J.; Cui, Y.; Mirams, G. R. Evaluation of an in Silico Cardiac Safety Assay: Using Ion Channel Screening Data to Predict QT Interval Changes in the Rabbit Ventricular Wedge. *J. Pharmacol. Toxicol. Methods* **2013**, *68*, 88−96.
(50) Romero, L.; Carbonell, B.; Trenor, B.; Rodríguez, B.; Saiz, J.; Ferrero, J. M. Systematic Characterization of the Ionic Basis of Rabbit Cellular Electrophysiology Using Two Ventricular Models. *Prog. Biophys. Mol. Biol.* **2011**, *107*, 60−73.
(51) Zicha, S.; Moss, I.; Allen, B.; Varro, A.; Papp, J.; Dumaine, R.; Antzelevich, C.; Nattel, S. Molecular Basis of Species-Specific Expression of Repolarizing K^+ Currents in the Heart. *Am. J. Physiol. Heart Circ. Physiol.* **2003**, *285*, H1641−9.
(52) Li, Z.; Dutta, S.; Sheng, J.; Tran, P. N.; Wu, W.; Chang, K.; Mdluli, T.; Strauss, D. G.; Colatsky, T. Improving the in Silico Assessment of Proarrhythmia Risk by Combining HERG (Human Ether-à-Go-Go-Related Gene) Channel-Drug Binding Kinetics and Multichannel Pharmacology. *Circ.: Arrhythmia Electrophysiol.* **2017**, *10*, No. e004628.
(53) Costabal, F. S.; Matsuno, K.; Yao, J.; Perdikaris, P.; Kuhl, E. Machine Learning in Drug Development: Characterizing the Effect of 30 Drugs on the QT Interval Using Gaussian Process Regression, Sensitivity Analysis, and Uncertainty Quantification. *Comput. Methods Appl. Mech. Eng.* **2019**, *348*, 313−333.
(54) Lacerda, A. E.; Kuryshev, Y. A.; Chen, Y.; Renganathan, M.; Eng, H.; Danthi, S. J.; Kramer, J. W.; Yang, T.; Brown, A. M. Alfuzosin Delays Cardiac Repolarization by a Novel Mechanism. *J. Pharmacol. Exp. Ther.* **2008**, *324*, 427−433.
(55) Yang, T.; Chun, Y. W.; Stroud, D. M.; Mosley, J. D.; Knollmann, B. C.; Hong, C.; Roden, D. M. Screening for Acute Ikr Block Is Insufficient to Detect Torsades de Pointes Liability: Role of Late Sodium Current. *Circulation* **2014**, *130*, 224−234.
(56) Crumb, W. J., Jr.; Vicente, J.; Johannesen, L.; Strauss, D. G. An Evaluation of 30 Clinical Drugs against the Comprehensive in Vitro Proarrhythmia Assay (CiPA) Proposed Ion Channel Panel. *J. Pharmacol. Toxicol. Methods* **2016**, *81*, 251−262.
(57) Polak, S.; Wiśniowska, B.; Brandys, J. Collation, Assessment and Analysis of Literature in Vitro Data on HERG Receptor Blocking Potency for Subsequent Modeling of Drugs' Cardiotoxic Properties. *J. Appl. Toxicol.* **2009**, *29*, 183−206.
(58) Gomis-Tena, J.; Brown, B. M.; Cano, J.; Trenor, B.; Yang, P.-C.; Saiz, J.; Clancy, C. E.; Romero, L. When Does the IC 50 Accurately Assess the Blocking Potency of a Drug? *J. Chem. Inf. Model.* **2020**, *60*, 1779−1790.
(59) Li, Z.; Mirams, G. R.; Yoshinaga, T.; Ridder, B. J.; Han, X.; Chen, J. E.; Stockbridge, N. L.; Wisialowski, T. A.; Damiano, B.; Severi, S.; Morissette, P.; Kowey, P. R.; Holbrook, M.; Smith, G.; Rasmusson, R. L.; Liu, M.; Song, Z.; Qu, Z.; Leishman, D. J.; Steidl-Nichols, J.; Rodriguez, B.; Bueno-Orovio, A.; Zhou, X.; Passini, E.; Edwards, A. G.; Morotti, S.; Ni, H.; Grandi, E.; Clancy, C. E.; Vandenberg, J.; Hill, A.; Nakamura, M.; Singer, T.; Polonchuk, L.; Greiter-Wilke, A.; Wang, K.; Nave, S.; Fullerton, A.; Sobie, E. A.; Paci, M.; Musuamba Tshinanu, F.; Strauss, D. G. General Principles for the Validation of Proarrhythmia Risk Prediction Models: An Extension of the CiPA In Silico Strategy. *Clin. Pharmacol. Ther.* **2020**, *107*, 102−111.
(60) Romero, L.; Trenor, B.; Yang, P. C.; Saiz, J.; Clancy, C. E. In Silico Screening of the Impact of HERG Channel Kinetic Abnormalities on Channel Block and Susceptibility to Acquired Long QT Syndrome. *J. Mol. Cell. Cardiol.* **2015**, *87*, 271−282.
(61) Milnes, J. T.; Witchel, H. J.; Leaney, J. L.; Leishman, D. J.; Hancox, J. C. Investigating Dynamic Protocol-Dependence of HERG Potassium Channel Inhibition at 37°C: Cisapride versus Dofetilide. *J. Pharmacol. Toxicol. Methods* **2010**, *61*, 178−191.
(62) di Veroli, G. Y.; Davies, M. R.; Zhang, H.; Abi-Gerges, N.; Boyett, M. R. hERG Inhibitors with Similar Potency but Different Binding Kinetics Do Not Pose the Same Proarrhythmic Risk: Implications for Drug Safety Assessment. *J. Cardiovasc. Electrophysiol.* **2014**, *25*, 197−207.
(63) Brown, C. S.; Farmer, R. G.; Soberman, J. E.; Eichner, S. F. Pharmacokinetic Factors in the Adverse Cardiovascular Effects of Antipsychotic Drugs. *Clin. Pharmacokinet.* **2004**, *43*, 33−56.
(64) van Noord, C.; Dieleman, J. P.; van Herpen, G.; Verhamme, K.; Sturkenboom, M. C. J. M. Domperidone and Ventricular Arrhythmia or Sudden Cardiac Death: A Population-Based Case-Control Study in the Netherlands. *Drug Saf.* **2010**, *33*, 1003−1014.
(65) Wiśniowska, B.; Polak, S. Am I or Am I Not Proarrhythmic? Comparison of Various Classifications of Drug TdP Propensity. *Drug Discovery Today* **2017**, *22*, 10−16.

https://dx.doi.org/10.1021/acs.jcim.0c00201
J. Chem. Inf. Model. 2020, 60, 5172−5187